International Geology Review

ISSN: 0020-6814 (Print) 1938-2839 (Online) Journal homepage: http://www.tandfonline.com/loi/tigr20

Extrusion vs. duplexing models of Himalayan mountain building 3: duplexing dominates from the Oligocene to Present

Dian He, A. Alexander G. Webb, Kyle P. Larson, Aaron J. Martin & Axel K. Schmitt

To cite this article: Dian He, A. Alexander G. Webb, Kyle P. Larson, Aaron J. Martin & Axel K. Schmitt (2015) Extrusion vs. duplexing models of Himalayan mountain building 3: duplexing dominates from the Oligocene to Present, International Geology Review, 57:1, 1-27, DOI: 10.1080/00206814.2014.986669

To link to this article: http://dx.doi.org/10.1080/00206814.2014.986669

International Geology Review, 2015
Vol. 57, No. 1, 1–27, http://dx.doi.org/10.1080/00206814.2014.986669

Taylor & Francis
Taylor & Francis Group

Extrusion vs. duplexing models of Himalayan mountain building 3: duplexing dominates from the Oligocene to Present

Dian He[a]*[†], A. Alexander G. Webb[a], Kyle P. Larson[b], Aaron J. Martin[c] and Axel K. Schmitt[d]

[a]*Department of Geology and Geophysics, Louisiana State University, Baton Rouge, LA, USA;* [b]*Earth and Environmental Sciences, University of British Columbia Okanagan, Kelowna, BC, Canada;* [c]*Department of Geology, University of Maryland, College Park, MD, USA;* [d]*Department of Earth, Planetary, and Space Sciences, University of California, Los Angeles, CA, USA*

(*Received 11 June 2014; accepted 8 November 2014*)

The Himalaya is a natural laboratory for studying mountain-building processes. Concepts of extrusion and duplexing have been proposed to dominate most phases of Himalayan evolution. Here, we examine the importance of these mechanisms for the evolution of the Himalayan crystalline core via an integrated investigation across the northern Kathmandu Nappe. Results reveal that a primarily top-to-the-north shear zone, the Galchi shear zone, occurs structurally above and intersects at depth with the Main Central thrust (MCT) along the northern flank of the synformal Kathmandu Nappe. Quartz *c*-axis fabrics confirm top-to-the-north shearing in the Galchi shear zone and yield a right-way-up deformation temperature field gradient. U-Pb zircon dating of pre-to-syn- and post-kinematic leucogranites demonstrates that the Galchi shear zone was active between 23.1 and 18.8 Ma and ceased activity before 18.8–13.8 Ma. The Galchi shear zone is correlated to the South Tibet detachment (STD) via consistent structural fabrics, lithologies, metamorphism, and timing for four transects across the northern margin of the Kathmandu Nappe. These findings are synthesized with literature results to demonstrate (1) the broad horizontality of the STD during motion and (2) the presence of the MCT-STD branch line along the Himalayan arc. The branch line indicates that the crystalline core was emplaced at depth via tectonic wedging and/or channel tunnelling-type deformation. We proceed to consider implications for the internal development of the crystalline core, particularly in the light of discovered tectonic discontinuities therein. We demonstrate the possibility that the entire crystalline core may have been developed via duplexing without significant channel tunnelling, thereby providing a new end-member model. This concept is represented in a reconstruction showing Himalayan mountain-building via duplexing from the Oligocene to Present.

Keywords: Himalayan orogen; Kathmandu Nappe; duplexing; extrusion

1. Introduction

The Himalaya (Figure 1) is one of the best natural laboratories for studying mountain-building processes. Extrusion and duplexing processes are invoked to address a series of Himalayan tectonic questions, including how ongoing mountain-building proceeds, and how the crystalline core developed and was emplaced (e.g. McElroy *et al.* 1990; Hodges *et al.* 2004; Webb *et al.* 2007; Herman *et al.* 2010; Martin *et al.* 2010; Corrie and Kohn 2011). In these contexts, extrusion involves exhumation from the middle crust of the over-riding plate to the surface between surface-breaching faults, commonly between an out-of-sequence thrust fault and a structurally higher normal fault, whereas duplexing involves basal accretion of material from the underthrusting Indian plate to the over-riding orogen. Models to explain the thermo-kinematic evolution from the late Miocene to Present generally involve either extrusion via out-of-sequence thrusting with or without structurally higher normal faulting (e.g. Harrison *et al.* 1997, 1998; Upreti and Le Fort 1999; Catlos *et al.* 2001, 2004; Hodges *et al.* 2001, 2004; Hurtado *et al.* 2001; Johnson *et al.* 2001; Wobus *et al.* 2003, 2005; Thiede *et al.* 2004; McDermott *et al.* 2013) or duplex development above a ramp in the sole thrust at mid-crust depth (e.g. DeCelles *et al.* 2001; Robinson *et al.* 2003; Bollinger *et al.* 2004, 2006; Konstantinovskaia and Malavieille 2005; Avouac 2007; Bhattacharyya and Mitra 2009; Herman *et al.* 2010; Long *et al.* 2011; Grandin *et al.* 2012; Adams *et al.* 2013; Webb 2013). Early to middle Miocene emplacement of the crystalline core has long been understood in the context of extrusion to the surface between the Main Central thrust (MCT) and South Tibet detachment (STD) (Figure 2A and B) (e.g. Caby and Le Fort 1983; Burg *et al.* 1984; Burchfiel and Royden 1985; Burchfiel *et al.* 1992; Hodges *et al.* 1992, 2001; Beaumont *et al.* 2001, 2004). However, over the past ~13 years, duplexing models have been considered for some of this emplacement history (e.g. Beaumont *et al.* 2001, 2004; Yin 2006; Larson *et al.* 2010b, 2013), or even all of this emplacement history (Figure 2C) (e.g. Webb *et al.* 2007,

*Corresponding author. Email: dian.he@shell.com
[†]Current address: Shell International Exploration and Production Inc., Houston, TX 77082, USA
This article was originally published with errors. This version has been corrected. Please see Corrigendum (http://dx.doi.org/10.1080/00206814.2015.1005906).

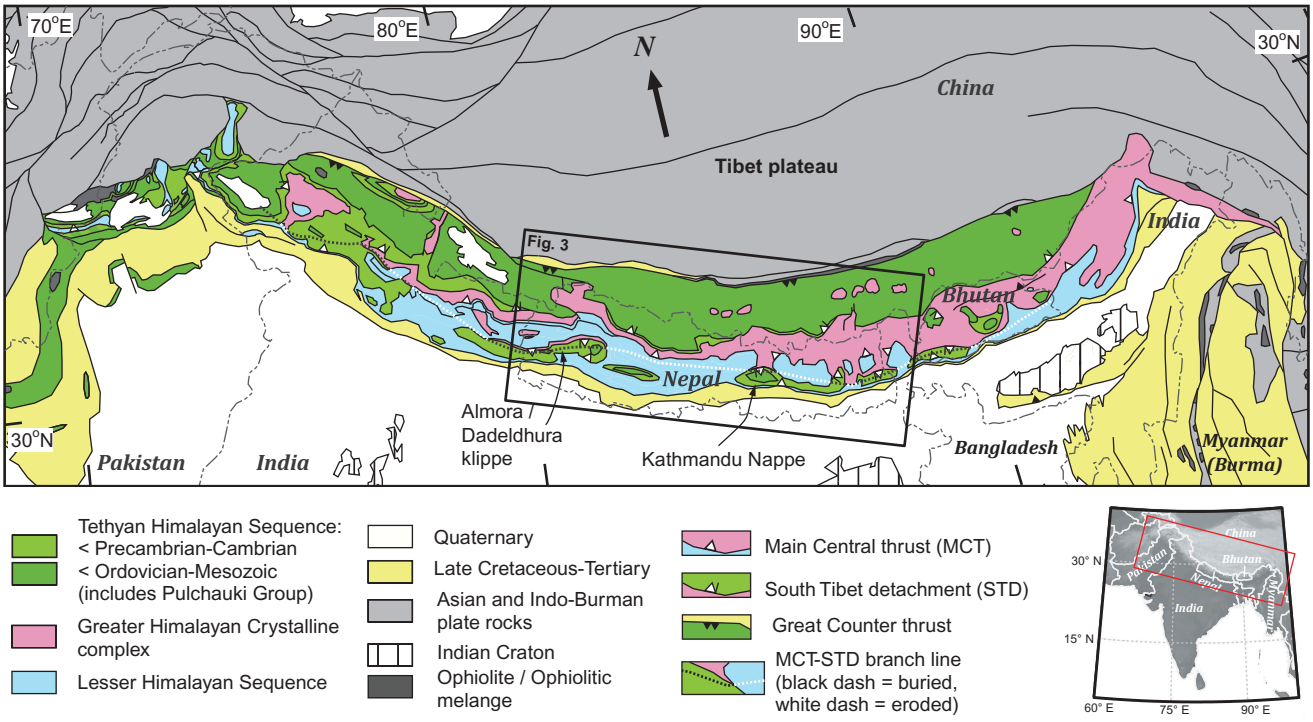

Figure 1. Simplified tectonic map of the Himalayan orogen, modified and integrated from Lombardo *et al.* (1993), Goscombe and Hand (2000), Murphy *et al.* (2009), Webb *et al.* (2011a, 2011b), and references therein. The inset of shaded relief map in the lower right corner shows the geographic context and the extent of this main map outlined by the red box. The black box in the main map shows the extent of Figure 3.

2011a, 2011b, 2013). More recently, as detailed exploration of the crystalline core has led to recognition of internal shear zones, the kinematics of crystalline core assembly has also been explained via both extrusion (e.g. Reddy *et al.* 1993; Carosi *et al.* 2007, 2010; Imayama *et al.* 2012; Mukherjee *et al.* 2012; Montomoli *et al.* 2013; Rubatto *et al.* 2013; Wang *et al.* 2013) and duplexing processes (Figure 2D) (e.g. Reddy *et al.* 1993; Martin *et al.* 2010; Corrie and Kohn 2011; Webb *et al.* 2013; Larson and Cottle 2014).

The central Nepalese Himalaya (Figure 3) has long served as the primary laboratory for exploration of the above questions. Nepal's open-access policy, dating to the 1950s, and the region's centrality in the Himalayan arc has led scores of international and Nepali geologists to conduct detailed investigations of the areas surrounding Kathmandu (as reviewed by Upreti 1999). Many important contributions of geological mapping and data sets have been produced, such that knowledge of this area has continually outpaced understanding of the remainder of the orogen (e.g. Hagen 1969; Le Fort 1975; Stöcklin 1980; Stöcklin and Bhattarai 1982; Arita 1983; Colchen *et al.* 1986; Pecher 1989; Hodges *et al.* 1996; Parrish and Hodges 1996; Bilham *et al.* 1997; Godin *et al.* 1999; DeCelles *et al.* 2000; Lavé and Avouac 2000; Burbank *et al.* 2003; Gehrels *et al.* 2003, 2006; Bollinger *et al.* 2004; Wobus *et al.* 2005; Herman *et al.* 2010; Grandin *et al.* 2012; Khanal and Robinson 2013; Khanal *et al.* 2014). The classical three-layer, two-fault structural stack geometry of the orogen – i.e. the crystalline core in fault contact with lower grade strata along both the MCT and STD – is well exposed and accessible along many parallel river transects here (Figure 3). Moreover, amphibolite facies rocks and subgreenschist facies rocks both extend from hinterland to foreland in nearly continuous exposures, enabling interrogation of the geological evolution via a broad range of techniques. The combination of the apparent simplicity of the structural pattern and the viability of many investigative techniques has regularly attracted cutting-edge analytical campaigns to the region (e.g. Macfarlane 1993; Parrish and Hodges 1996; Rai *et al.* 1998; Catlos *et al.* 2001; Johnson *et al.* 2001; Beyssac *et al.* 2004; Bollinger *et al.* 2004; Kohn *et al.* 2004; Law *et al.* 2004; Carosi *et al.* 2006; Blythe *et al.* 2007; Larson and Godin 2009; Herman *et al.* 2010).

A recently proposed modification to the structural framework of the central Nepal Himalaya would alter our understanding of the extrusion and duplexing models for the emplacement of the crystalline core. Namely, Webb *et al.* (2011a) suggested that the southern portion of the STD intersects the MCT, thus bounding the southern limit of the crystalline core. Because the posited MCT–STD intersection geometry implies that the leading edge of the

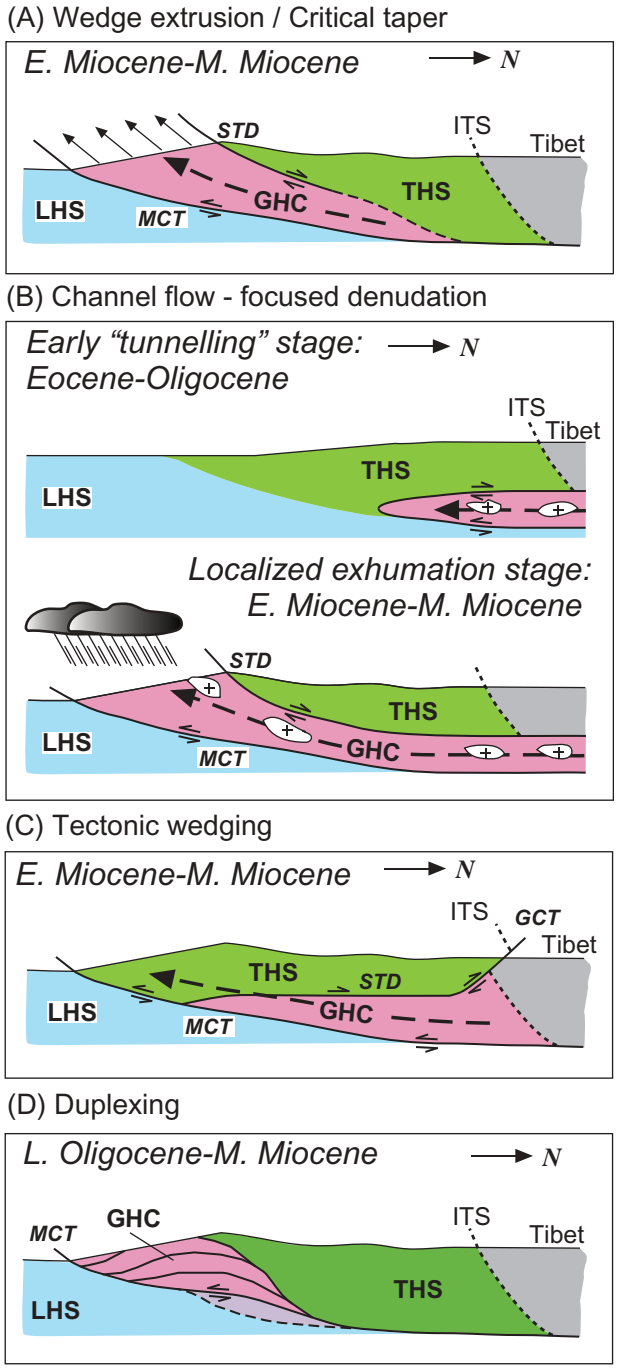

Figure 2. Himalayan tectonic models for development and emplacement of the Greater Himalayan Crystalline complex modified from Webb *et al.* (2011a). In the classification of this study (extrusion vs. duplexing), model (A) is extrusion, models (C) and (D) are duplexing, and the early channel tunnelling stage of model (B) is duplexing and the later localized exhumation stage is extrusion. See text for details. LHS, Lesser Himalayan Sequence; GHC, Greater Himalayan Crystalline complex; THS, Tethyan Himalayan Sequence; MCT, Main Central thrust; STD, South Tibet detachment; GCT, Great Counter thrust; ITS, Indus-Tsangpo suture.

crystalline core is buried today and then requires the crystalline core to have been emplaced at depth, it challenges long-standing Himalayan extrusion models. However, the initial study by Webb *et al.* (2011a) only presented evidence of this southern STD geometry from a single locality approximately 50 km northwest of Kathmandu (Figure 3). There appears to be compelling evidence in the central Nepal Himalaya, but it has as yet been documented at only one site. Their model makes firm predictions for other sites, given the geometry of the claimed discovery site, so we test these predictions by looking at more sites.

In this study, we address this problem via field-based investigation integrating kinematic analysis, quartz *c*-axis fabric analysis, and U-Pb geochronology along the proposed trace of the STD in the Kathmandu region. Our results confirm that the STD occurs across the region and intersects with the MCT to the south. Similar results obtained in the Dadeldhura klippe of western Nepal are presented in a companion paper (He *et al.* 2014). We then discuss the implications of the revised STD geometry for crystalline core emplacement and development models. Finally, by integrating our new work with existing constraints on other aspects of Himalayan development, we present a kinematic model showing that Himalayan mountain-building processes have been dominated by duplexing since the Oligocene or earlier.

2. Geology of the Kathmandu Nappe

Variably metamorphosed (half-)klippen along the southern portions of the Himalayan arc such as the Kathmandu Nappe (precisely: half-klippe) do not have a generally accepted position within the tectonic framework of the Himalayan orogen (e.g. Upreti and Le Fort 1999; Johnson 2005; Webb *et al.* 2011a). These rocks have been interpreted as belonging to one or more of the three major units in the orogenic wedge: the Lesser Himalayan Sequence, the Greater Himalayan Crystalline complex, and the Tethyan Himalayan Sequence. These three units are commonly defined as fault-separated, that is, the Greater Himalayan Crystalline complex is bounded by the MCT below and the STD above, the Lesser Himalayan Sequence is the MCT footwall, and the Tethyan Himalayan Sequence occupies the STD hanging wall (e.g. Upreti 1999; Hodges 2000; Yin 2006; Searle *et al.* 2008; cf. Long and McQuarrie 2010).

The Kathmandu Nappe is located in central Nepal with Kathmandu city near its centre (Figure 3). It was emplaced to the south along the Mahabharat thrust, which is widely interpreted as the southern strand of the MCT (e.g. Stöcklin 1980; Johnson *et al.* 2001). Subsequent accretion

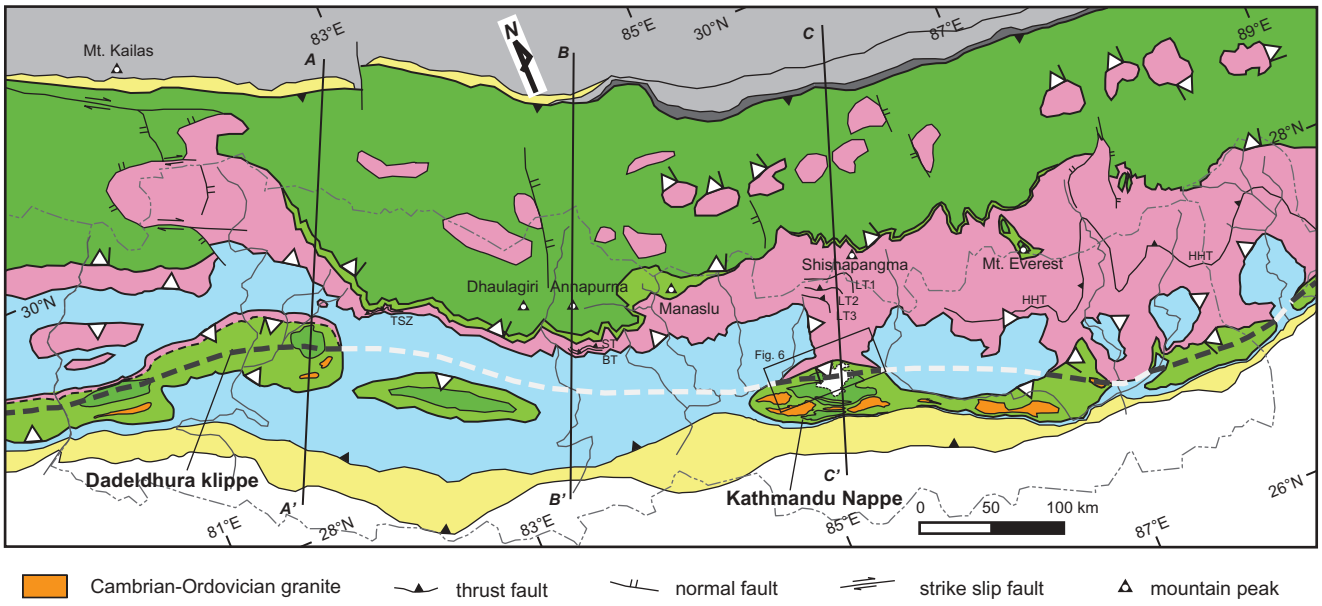

Figure 3. Simplified geological map of the central Himalaya, units as in Figure 1 except as specified. Three lines of cross sections A-A′, B-B′, and C-C′ are present in Figure 4; the area of Figure 6 is outlined. This map is based on integration of the following works: Gurla Mandhata–Lower Dolpo region in west Nepal modified from Murphy and Copeland (2005), Carosi *et al.* (2007, 2010); Dhaulagiri–Annapurna–Manaslu region modified from Hodges *et al.* (1996), Vannay and Hodges (1996), Searle and Godin (2003), Martin *et al.* (2005); Shishapangma–Everest–Ama Drime region modified from Searle *et al.* (1997, 2003, 2008), Cottle *et al.* (2007), Kali *et al.* (2010); Dadaldhura klippe region modified from Hayashi *et al.* (1984), Upreti (1999), DeCelles *et al.* (2001), Robinson *et al.* (2006), Célérier *et al.* (2009); Kathmandu region modified from Stöcklin and Bhattarai (1982), Rai *et al.* (1998), Johnson *et al.* (2001), Gehrels *et al.* (2006), Webb *et al.* (2011a), and our mapping; eastern Nepal and its easterly region modified from Lombardo *et al.* (1993), Goscombe and Hand (2000), Grujic *et al.* (2011), Kellett and Grujic (2012); North Himalaya gneiss domes region modified from Lee *et al.* (2004), Quigley *et al.* (2006), Larson *et al.* (2010a), Wagner *et al.* (2010), King *et al.* (2011), Zhang *et al.* (2012); Indus–Yalu suture zone modified from Murphy *et al.* (2009), Webb *et al.* (2011a). TSZ, Toijem shear zone (Carosi *et al.* 2010); BT, Bhanuwa thrust, ST, Sinuwa thrust (Corrie and Kohn 2011); LT1, LT2, LT3, Langtang thrusts 1, 2, 3 (Reddy *et al.* 1993); HHT, High Himal thrust (Goscombe *et al.* 2006).

of underlying Lesser Himalayan material warped the nappe into its current geometry: a bowl-shaped synformal, elongated in the arc-parallel direction (Figure 4; e.g. Brunel 1986; Bollinger *et al.* 2004). The nappe rocks of the hanging wall are dominated by the Bhimphedi Group, Phulchauki Group, and Sheopuri Gneiss (Stöcklin 1980; Upreti 1999). The Bhimphedi Group is composed of late Proterozoic medium- to high-grade metasedimentary rocks intruded by Cambrain–Ordovician granites, which are unconformably overlain by the Phulchauki Group, a section of Ordovician–Devonian low-grade and unmetamorphosed sedimentary rocks (e.g. Stöcklin 1980; Upreti and Le Fort 1999; DeCelles *et al.* 2000; Johnson *et al.* 2001; Gehrels *et al.* 2003, 2006). The Phulchauki Group is commonly correlated to the Tethyan Himalayan Sequence rocks of the same ages (e.g. Stöcklin 1980; Johnson *et al.* 2001; Gehrels *et al.* 2006), whereas the affiliation of the Bhimphedi Group remains debated (see next paragraph). The Bhimphedi–Phulchauki succession is characterized by a right-way-up thermal gradient peaking at ~650°C along the top of the ~1–2 km-thick basal shear zone; the basal shear zone itself displays an inverted metamorphic field gradient down to ~300°C (Johnson *et al.* 2001). This metamorphic pattern contrasts with the famed inverted metamorphic field gradient that extends not just across the major trace of the MCT but also throughout most of the Greater Himalayan Crystalline complex. Sections crossing the crystalline core to the north generally show higher metamorphic temperatures with increasing structural elevation (e.g. cf. Johnson *et al.* 2001 vs. Le Fort 1975). The Sheopuri Gneiss, correlative to the Greater Himalayan Crystalline complex, occurs along the northern margin of the Kathmandu Nappe (e.g. Rai *et al.* 1998; Johnson *et al.* 2001). This unit largely consists of kyanite/sillimanite-bearing migmatitic gneiss and schist (Rai *et al.* 1998).

Four models may explain the architecture of the Kathmandu Nappe and potential correlations of nappe rocks across the orogen (Figure 5): (1) The STD occurs within the Bhimphedi Group such that the lower Bhimphedi Group is the southern continuation of the Greater Himalayan Crystalline complex (Yin 2006). The upper Bhimphedi Group and Phulchauki Group together are the Tethyan Himalayan Sequence above the southerly

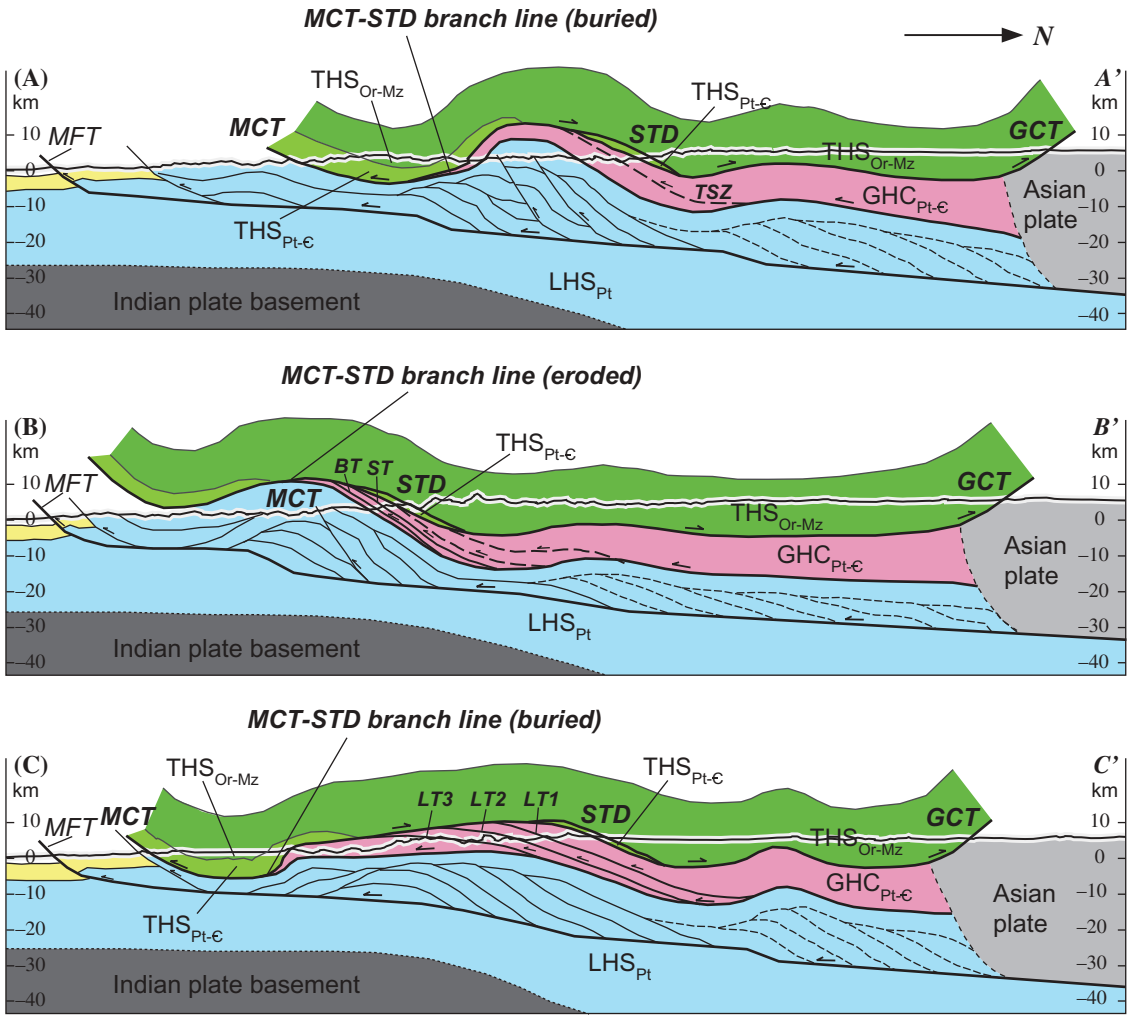

Figure 4. Schematic cross sections of the central Himalayan orogen across the Dadeldhura klippe (A-A′), Annapurna region (B-B′), and Kathmandu region (C-C′). The Tethyan Himalayan Sequence is highly simplified; the deeper duplex system (dashed lines) in the Lesser Himalayan Sequence is a model for the formation of the North Himalayan Gneiss domes (Murphy 2007). The characteristics of the units are based on following articles: the Tethyan Himalayan Sequence after Godin *et al.* (2001), Godin (2003), Kellett and Godin (2009), Searle (2010); the Greater Himalayan Crystalline complex after Inger and Harris (1992), Vannay and Hodges (1996), Beaumont *et al.* (2001), Grujic *et al.* (2002), Jamieson *et al.* (2004); the internal structures of the Greater Himalayan Crystalline complex after Reddy *et al.* (1993), Carosi *et al.* (2010), Corrie and Kohn (2011); the Lesser Himalayan Sequence duplex after Bollinger *et al.* (2006), Robinson *et al.* (2006), Murphy (2007), Herman *et al.* (2010); the frontal klippen after Upreti and Le Fort (1999), Webb *et al.* (2011a), and this study. MFT, Main Frontal thrust.

STD (Figure 5A). (2) The STD does not occur in the nappe and all rocks in the nappe are in the footwall of the STD (Johnson *et al.* 2001; Gehrels *et al.* 2003; Robinson *et al.* 2003). In this model, the Bhimphedi Group is the southern continuation of the Greater Himalayan Crystalline complex; the Phulchauki Group is stratigraphically correlative to coeval Tethyan Himalayan Sequence rocks but is nonetheless part of the STD footwall (Figure 5B). In this model, the contact of the Bhimphedi-Sheopuri groups is an unconformity or a second-order faulting contact. (3) The Kathmandu Nappe is a separate thrust sheet (vs. the MCT thrust sheet) carried by the Mahabharat thrust in the MCT footwall (Rai *et al.* 1998; Upreti and Le Fort 1999; Hodges 2000). The Bhimphedi Group is consequently interpreted as the Lesser Himalayan Sequence rocks; interpretation of the Phulchauki Group is similar to that in model 2 (Figure 5C). This model predicts that the contact of the Sheopuri Gneiss and the Bhimphedi Group rocks along the northern margin of the Kathmandu Nappe is the top-to-the-south MCT shear zone. Note that this model conflicts with the dominant interpretation that the Mahabharat thrust is the MCT. (4) The STD occurs along the northern margin of the Kathmandu Nappe. To the south the STD merges with the MCT to form a branch line (Webb *et al.* 2011a). Both the Bhimphedi Group and Phulchauki Group are

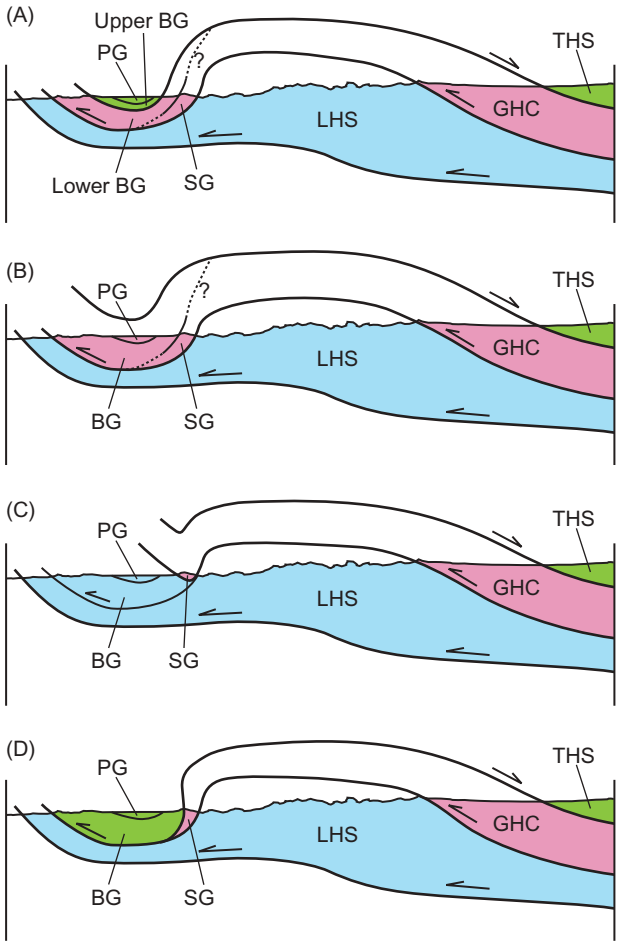

Figure 5. Structural models of the Kathmandu Nappe. Representative papers of each model are: (A) Yin (2006); (B) Johnson *et al.* (2001), Gehrels *et al.* (2003), Robinson *et al.* (2003); (C) Rai *et al.* (1998), Upreti and Le Fort (1999), Hodges (2000), and (D) Webb *et al.* (2011a). BG, Bhimphedi Group; PG, Phulchauki Group; SG, Sheopuri Gneiss. See text for details.

correlative to the Tethyan Himalayan Sequence in that the Bhimphedi–Phulchauki succession is located to the south of the MCT–STD branch line and in the hanging walls of both faults (Figure 5D; e.g. Webb *et al.* 2007; Webb *et al.* 2011a). The buried southern limit of the Sheopuri Gneiss, defined by the branch line, likewise represents the southern limit of the Greater Himalayan Crystalline complex. Therefore in contrast to the third model, this model predicts that the contact of the Sheopuri Gneiss and the Bhimphedi Group rocks along the northern margin of the Kathmandu Nappe is the top-to-the-north STD shear zone. In contrast, recent studies by Sapkota and Sanislav (2013) interpret the top-to-the-north shearing signals in this area as a set of youngest (post-MCT) structures resulting from reactivation of older top-to-the-south shearing structures during folding of the Kathmandu Nappe. In this contribution, we test the models by investigating this contact along the northern margin of the Kathmandu Nappe.

Geochronological work provides some constraints on the timing of the emplacement and deformation of the Kathmandu Nappe. Th-Pb ages of monazite inclusions in garnet crystals from the Bhimphedi Group and U-Pb zircon ages of cross-cutting granites in the Bhimphedi Group indicate that the frontal klippen experienced early Palaeozoic tectonism (Gehrels *et al.* 2003, 2006). Johnson *et al.* (2001) obtained a U-Pb zircon age of ~18 Ma from a syn-kinematic leucogranite near the Sheopuri-Bhimphedi contact. A leucogranite along the contact which is deformed by top-to-the-north C′ shear bands yielded U-Pb zircon ages as young as 20 Ma (Webb *et al.* 2011a). $^{40}Ar/^{39}Ar$ muscovite cooling ages from the Kathmandu Nappe decrease from ~22 Ma at the southern margin to as young as ~12 Ma at the northern margin of the synform (Arita *et al.* 1997; Bollinger *et al.* 2006; Herman *et al.* 2010). Similarly, Rb/Sr mica cooling ages range from 22 to 14 Ma across the nappe (Johnson and Rogers 1997). These Miocene ages indicate that emplacement of the Kathmandu Nappe along its ductile basal shear zone was completed by ~14 Ma.

3. Structural geology

Here, we present results of new structural mapping across the Sheopuri Gneiss–Bhimphedi Group contact along the northern limit of the Kathmandu Nappe synform (Figure 6). We previously reported results of similar work along a single transect across this contact along the Mahesh Khola (i.e. Mahesh River) (see Webb *et al.* 2011a). Four additional transects across the contact are investigated in this study: the Kakani, Chisapani, Lapsephedi, and Lamidanda transects from west to east. Together, these five transects represent coverage of the entire northern Kathmandu Nappe synform (Figure 6). In general, the Sheopuri-Bhimphedi contact across these transects is marked by a southward change from kyanite-bearing gneiss, garnet mica schist, granitic gneiss, and calc-silicate gneiss to quartzite, biotite schist, marble, and weakly deformed (and apparently undeformed) granites.

Our prior effort benefitted from continuous fresh rock exposure across the contact due to fluvial erosion by the Mahesh Khola. In contrast, exposure along the new transects is generally limited to modest roadcuts and is altered by intensive farming. Only patchy records can be observed, so that the N–S extent of the Sheopuri-Bhimphedi contact is hardly constrained along these transects. Poor rock quality, even at the freshest roadcuts, indicates that weathering processes here reach many metres, and perhaps tens of metres, into the hillsides.

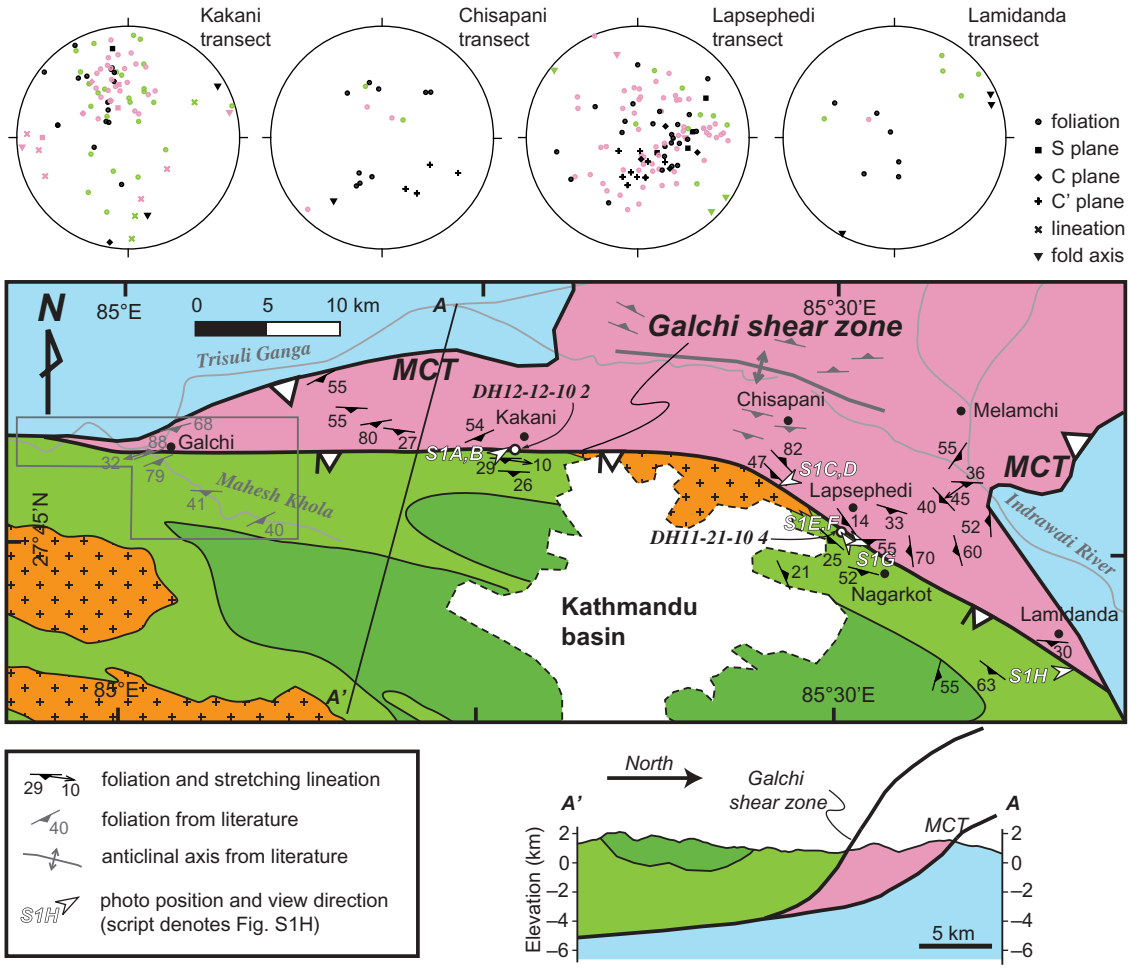

Figure 6. Geological map and a cross section of the northern Kathmandu Nappe, units as in Figure 3, except as specified. The stereonets show the structure data from each transect, respectively. The colour code is the same as the units on the map, except that the black represents the data from the Galchi shear zone. Modified from Rai *et al.* (1998), Johnson *et al.* (2001), Gehrels *et al.* (2006), Webb *et al.* (2011a), and this study. Structural data in grey along the Mahesh Khola are from Webb *et al.* (2011a) and those in the northern part of the Nappe are from Rai *et al.* (1998).

Due to this aggressive weathering, much of the rock is altered and linear fabrics are commonly obliterated, but planar rock fabrics are generally preserved. Variable manifestations of the deformation features along different transects also may be partially a response to the weathering.

The Kakani transect extends along a farm-lined highway from Kathmandu through Kakani. Exposures in the vicinity of the Sheopuri–Bhimphedi contact here are characterized by quartzofeldspathic gneisses and calc-silicate gneisses deformed in tight asymmetric folds (Figures S1A, S1B). The width of the contact is constrained to be <400 m on the basis of first appearances of the Sheopuri and Bhimphedi units to the north and south, respectively. The fold asymmetry consistently yields a top-to-the-north vergence, consistent with observed shear senses at other locales as explained in the following paragraphs. Rocks north of the contact zone are dominantly gneisses, garnet mica schists, and deformed granites; south of this highly deformed exposure quartzites and low-grade metamorphosed pelitic schists intruded by undeformed granites occur. These two rock assemblages are consistent with descriptions of the Sheopuri Gneiss and the Bhimphedi Group, respectively (e.g. Stöcklin 1980; Upreti and Le Fort 1999; Gehrels *et al.* 2006). Prior mapping by Stöcklin and Bhattarai (1982) shows the Sheopuri Gneiss–Bhimphedi Group contact at the same position along this transect.

The Chisapani transect follows a road across a jungle area from Kathmandu to Chisapani. The Sheopuri–Bhimphedi contact along this transect occurs ~5 km south of Chisapani with estimated width of <500 m (again on the basis of first appearances of the Sheopuri and Bhimphedi units to the north and south, respectively). The contact features quartzofeldspathic gneisses and calc-silicate gneisses, both intruded by metre-scale leucogranite

dikes, all deformed by metre-scale asymmetric boudinage (Figures S1C, S1D). The asymmetric boudinage consistently displays a top-to-the-north sense of shear (average dip direction/dip of the shear band surfaces: 314°/49°; see stereonet in Figure 6). The contact separates quartzofeldspathic gneisses characterized by gneissic banding to the north from weakly deformed and apparently undeformed granites to the south. These rocks are correlated to the Sheopuri Gneiss and Cambrian–Ordovician granites of the Bhimphedi Group, respectively (e.g. Stöcklin and Bhattarai 1982; Gehrels *et al.* 2006).

The Lapsephedi transect covers the farming region spanning Nagarkot, Melamchi, and Lapsephedi to the northeast of Kathmandu. We encountered the Sheopuri-Bhimphedi contact twice along its strike during a loop transect. The contact thickness is poorly constrained here and can only be estimated as <1300 m (on the basis of first appearances of the Sheopuri and Bhimphedi units to the north and south, respectively). One exposure of the shear zone is characterized by asymmetric boudinage that deforms leucogranitic lenses and gneissic bands (Figures S1E, S1F). The other, ~3 km to the southeast, features sigma-type feldspar porphyroclasts in granitic gneisses (Figure S1G). The asymmetric boudinage and sigma-type porphyroclasts both display top-to-the-north sense of shear (average dip direction/dip of the shear band surfaces: 0°/25°). Rocks north of the contact are mainly composed of granitic gneisses, quartzites, kyanite-bearing paragneisses, and garnet biotite gneisses; rocks south of the contact are dominantly low-grade biotite schists with minor occurrences of apparently undeformed tourmaline two-mica granites. The northern rocks display foliation, S-C fabrics, boudinage, and isoclinal folds, but this deformation appears less concentrated in contrast with the contact shear zone.

The Lamidanda transect is the easternmost transect examined. The Sheopuri–Bhimphedi contact along this transect is characterized by strongly folded schists. The contact has a poorly constrained width estimation of <2500 m due to limited access to exposures. S-shaped folds and recumbent folds in the schists are abundant in an exposure ~3 km south of Lamidanda (Figure S1H). The S-shaped folds are consistent with a top-to-the-north sense of shear, and the recumbent folds are north-vergent (average trend/plunge of the fold axes: 55°/3°; see stereonet in Figure 6). Quartzites and limestones are dominant to the southwest of this exposure and garnet mica schists and granitic gneisses are abundant to the northeast, corresponding to the Bhimphedi–Phulchauki Groups and Sheopuri Gneiss, respectively (e.g. Stöcklin 1980). Structural fabrics of the Bhimphedi rocks to the southwest include mica foliation, folding, and primary bedding, while the Sheopuri rocks to the northeast are dominated by mica foliation.

In summary, observations along the four transects demonstrate that the Sheopuri–Bhimphedi contact is characterized by a shear zone with consistent top-to-the-north shear sense. These findings are consistent with our prior work along the Mahesh Khola (Webb *et al.* 2011a), in which we termed this shear zone the Galchi shear zone. Taken together, our findings indicate that the Galchi shear zone spans the northern reaches of the Kathmandu Nappe synform.

4. Quartz *c*-axis fabrics

We employ quartz *c*-axis fabric analysis to characterize the shear-sense and deformation temperature experienced during movement across the Galchi shear zone. We conducted such analysis for three samples from the Mahesh Khola transect (Figure 7). Other transects that we mapped consist of highly weathered rocks (Figure S1), so that it is almost impossible to make thin sections for this type of analysis. Sample EW12-26-07 2B is garnet-bearing quartz leucosome, showing steeply dipping foliation to the south and stretching lineation to the south-southwest. Sample AW12-25-07 1B is quartzite with steeply south dipping foliation defined by mica. Sample AW12-24-07 8 is garnet-biotite schist with S-dipping foliation.

4.1. Methods

In deformed quartz-rich rocks, dynamically recrystallized quartz grains can develop a lattice-preferred orientation (LPO) in response to strain that is recorded by systematic *c*-axis orientations (e.g. Lister and Price 1978; Lister and Hobbs 1980; Schmid and Casey 1986; Law 1990). Quartz *c*-axis fabric analysis of our specimens was conducted using a Russell-Head Instruments G50 automated fabric analyser housed at the University of Saskatchewan. Quartz *c*-axis fabric analysis from similar or identical instruments has proved to be indistinguishable from those determined through electron back-scattered diffraction (e.g. Wilson *et al.* 2007; Peternell *et al.* 2010). All thin sections analysed were cut perpendicular to foliation and parallel to mineral stretching lineation and all *c*-axis orientation data are plotted in equal-area lower-hemisphere stereographic projection. The projection plane is perpendicular to foliation and parallel to lineation such that the lineation lies horizontal in the E–W direction and the foliation plane lies vertical in the same direction. Contour and scatter plots were generated using Stereonet 7.2.4 developed by R (W. Allmendinger 2012). All quartz *c*-axis fabric plots are viewed towards the east such that, for example, a sinistral asymmetric pattern with respect to foliation indicates a top-to-the-north sense of shear.

4.2. Results

Sample EW12-26-07 2B is from the Galchi shear zone in the Mahesh Khola area, whereas samples AW12-25-07 1B and AW12-24-07 8 are from the hanging wall of the shear

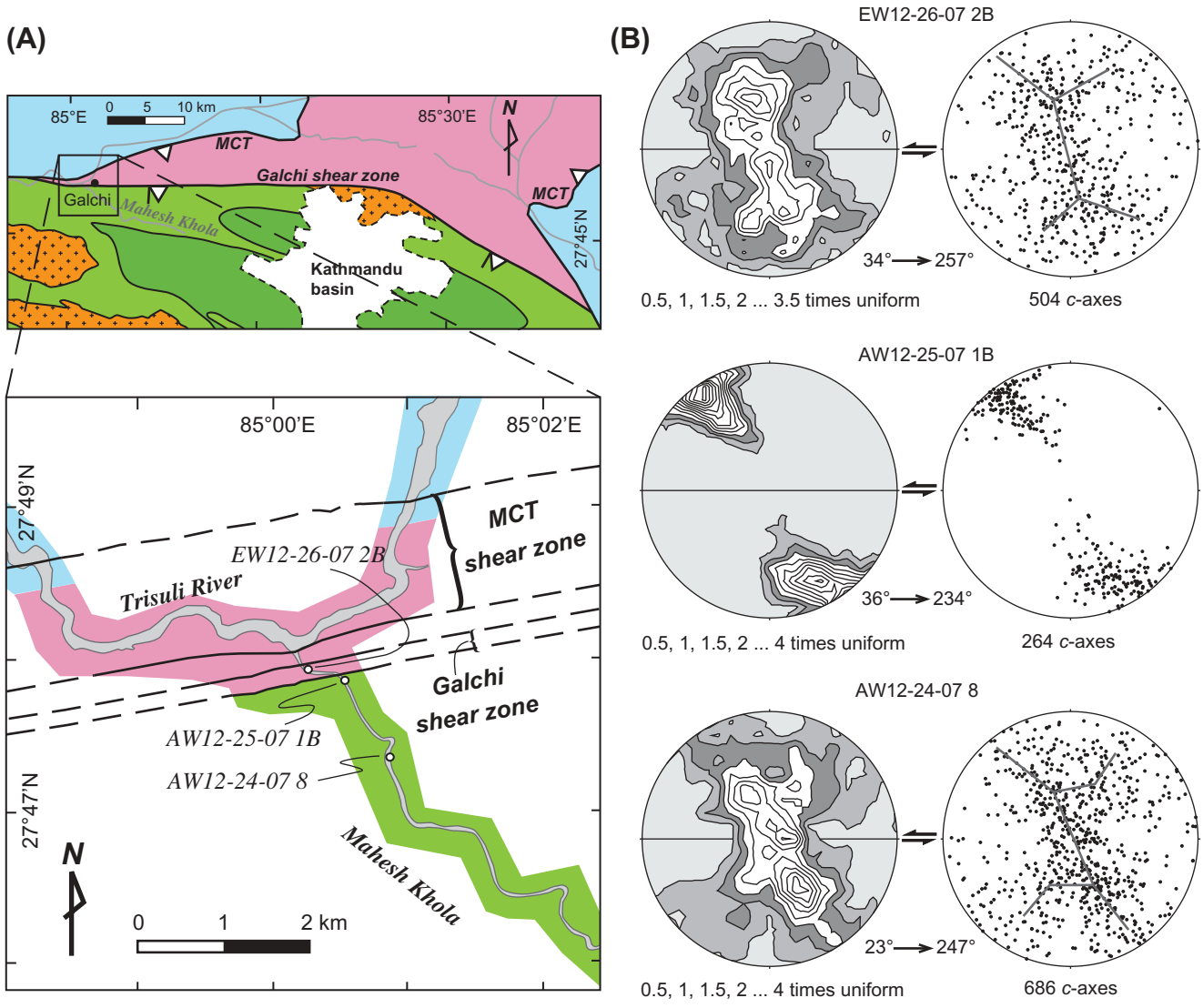

Figure 7. Quartz *c*-axis fabric patterns of samples from the Mahesh Khola transect in the Kathmandu Nappe. (A) Simplified geological map of the northern Kathmandu Nappe and the Mahesh Khola transect (modified from Webb *et al.* 2011a). (B) Quartz *c*-axis fabric diagram. Sample locations are marked in (A). All data are presented in lower-hemisphere equal-area projection and viewed towards the east. Plane of projection is perpendicular to foliation and parallel to lineation. Shear sense is indicated by half-arrows.

zone here (Figure 7A). The quartz LPO yielded by EW12-26-07 2B exhibits a poorly defined type-I cross-girdle fabric with an asymmetry consistent with top-to-the-northeast shear (Figure 7B). Sample AW12-25-07 1B yields a well-developed single girdle fabric that also has an asymmetry consistent with top-to-the-northeast shear. Sample AW12-24-07 8, the structurally highest specimen analysed from the Mahesh Khola transect, yields a poorly developed type-I cross-girdle LPO with an asymmetry that indicates top-to-the-northeast shear (Figure 7B). The asymmetry of all three samples is consistent with the field observations of Webb *et al.* (2011a) that indicate top-to-the-northeast shearing.

4.3. *Deformation temperature estimates*

Assuming a consistent critical resolved shear stress per sample and lack of hydrolytic weakening effects, the opening angles of quartz *c*-axis cross-girdle fabrics may be used to estimate the temperature at which they developed during deformation (Tullis *et al.* 1973; Lister and Hobbs 1980; Kruhl 1998; Law *et al.* 2004). Opening angles have been empirically shown to have an approximately linear relationship with deformation temperatures between ~300 and 650°C (Kruhl 1998; Law *et al.* 2004). This empirical calibration is subject to an estimated error of ±50°C to reflect both analytical and judgement-induced errors (Kruhl 1998). Many studies carried out across the

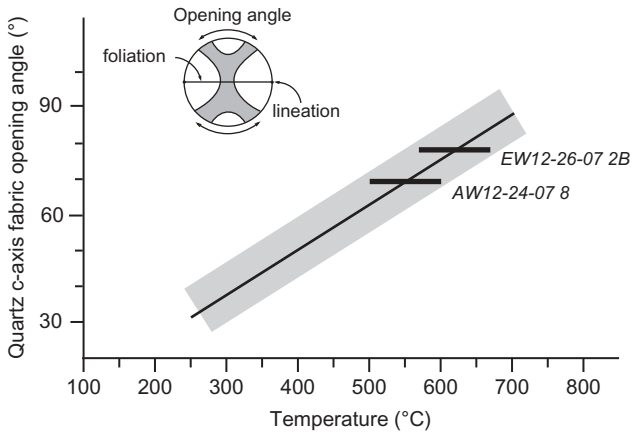

Figure 8. Empirical relationship between opening angles of quartz *c*-axis fabric patterns and deformation temperatures with samples from the Mahesh Khola transect in the Kathmandu Nappe, modified from Law *et al.* (2004). Grey bar represents ±50°C uncertainty. A conceptual *c*-axis fabric girdle on a stereonet is shown in the upper-left corner.

Himalayan orogen indicate that the deformation temperatures, across both the MCT and STD, estimated from fabric opening angles are comparable with the metamorphic temperatures derived by mineral assemblages (e.g. Law *et al.* 2004; Larson and Godin 2009; Larson *et al.* 2010a, 2010b, 2013; Law *et al.* 2011; Yakymchuk and Godin 2012; Law *et al.* 2013; Larson and Cottle 2014; see also review of Law, 2014). We therefore argue that the quartz *c*-axis fabric opening angle thermometer is applicable to our specimens and can make reasonable deformation temperature estimates.

Two of the samples analysed, EW12-26-07 2B and AW12-24-07 8, have type-I cross-girdled patterns that may be appropriate for deformation temperature estimation. The LPO patterns yield opening angles of 69° for AW12-24-07 8 and 78° for EW12-26-07 2B as measured about the top and bottom poles of the stereonets. Those opening angles indicate deformation temperatures of 550 ± 50°C for AW12-04-07 8 and 620 ± 50°C for EW12-26-07 2B (Figure 8). These temperatures are indistinguishable from peak metamorphic temperatures (686°C and 591°C) derived from garnet-biotite thermometry by Johnson *et al.* (2001) for rocks of the same areas.

5. U-Pb zircon geochronology

5.1. Methods

Two leucogranite samples from Galchi shear zone in the Kathmandu Nappe were analysed via U-Th-Pb zircon geochronology to determine timing of shearing. Fifty-eight spot data from 32 zircon grains were acquired using the CAMECA IMS 1270 ion microprobe at the University of California–Los Angeles. The detailed analytical procedure is described by Schmitt *et al.* (2003). The analyses were undertaken using an 8–15 nA O- primary beam with a ~15 μm diameter spot size, which generated a crater with ~1 μm depth. U-Pb ratios were determined using a calibration curve based on UO/U *versus* Pb/U from zircon standard AS3 with age of 1099.1 Ma (Paces and Miller 1993) and adjusted using common Pb for the late Cenozoic (Stacey and Kramers 1975). Concentrations of U were calculated by comparison with zircon standard 91500 with a U concentration of 81.2 ppm (Wiedenbeck 2004). Data reduction was accomplished by the in-house program ZIPS 3.0 developed by Chris Coath.

5.2. Results

Sample DH11-21-10 4 was collected south of Lapsephedi along the Lapsephedi transect from an undeformed leucogranite body that cross-cuts top-to-the-north fabrics of the Galchi shear zone (Figures 6 and S2A, S2C). Among the 24 spots analyses from 14 zircon grains, four spots yield early Palaeozoic $^{238}U/^{206}Pb$ ages from ca. 489 to 508 Ma (Figure 9 and Table S1). Note that the errors of all age data can be found in Table S1 and visualized in Figure 9. These older spot analyses have low U concentrations (332 ppm on average) and low U/Th ratios (2.25 on average). Cathodoluminescence (CL) images reveal that these early Palaeozoic ages are from grains characterized by bright colour, euhedral shapes, and small grain sizes (Figure 9A). The remaining 20 spot analyses exhibit concordant late Oligocene to middle Miocene $^{238}U/^{206}Pb$ ages with two clusters: grain core ages of ca. 26.7–19.3 Ma and grain rim ages of ca. 18.8–13.8 Ma (Figure 9B). Among these Cenozoic ages, the core ages have high U concentration (>5680 ppm) and high U/Th ratios (mostly >100), whereas the rim ages have lesser U concentrations (2295–3786 ppm) and U/Th ratios (37–80). CL images show that the cores with Cenozoic ages are characterized by mosaic textures, truncated by younger rims with convoluted zoning (Figure 9A).

Sample DH12-12-10 2 is from a deformed leucogranitic sill in the top-to-the-north Galchi shear zone in the vicinity of Kakani (Figure 6). The leucogranitic lens is concordant with foliation of the host rock and boudinaged (Figures S2B, S2D), indicating that it is pre-kinematic or syn-kinematic. Thirty-four spots from 18 zircon grains were analysed. Ten spot analyses are discordant and yield $^{238}U/^{206}Pb$ ages ranging from ca. 931 to 45.5 Ma; the remaining 24 spot analyses are concordant and yield $^{238}U/^{206}Pb$ ages of ca. 37.5–23.1 Ma (Figure 9 and Table S1). Among the younger ages, rim ages spread from ca. 30.8 to 23.1 Ma with an outlier age of 37.5 Ma, whereas cores yield ages of ca. 34.7–29.4 Ma (Figure 9B). Analyses yielding discordant data have low-U concentrations (mostly <2000 ppm) and low U/Th ratios (3.7–62),

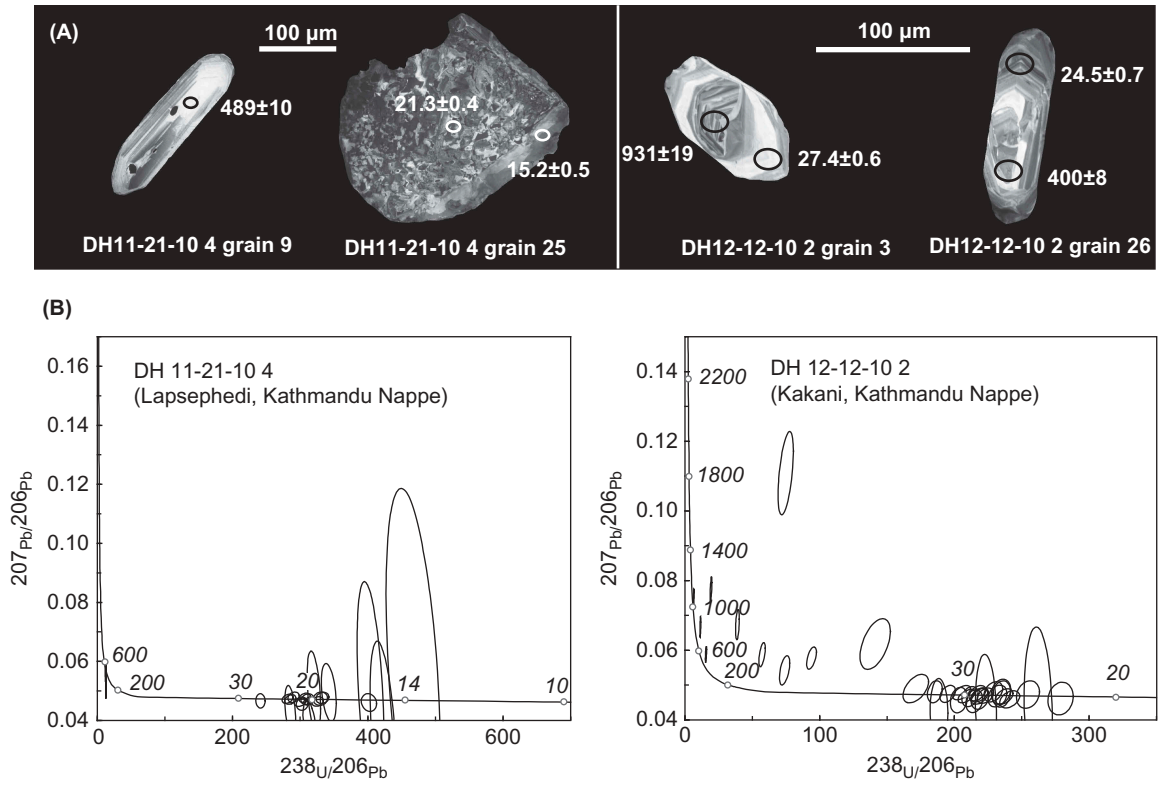

Figure 9. U-Pb zircon geochronology of leucogranite samples from the Galchi shear zone in the Kathmandu Nappe. (A) SEM cathodoluminescence (CL) images of representative zircon grains from two dated samples with $^{206}Pb/^{238}U$ ages. (B) Concordia diagram of U-Pb analyses. Sample locations are marked in Figure 6.

whereas the Cenozoic concordant ages have high-U concentrations (mostly >2000 ppm) and high U/Th ratio (mostly >100). CL images reveal that the discordant old ages correspond to bright, oscillatory-zoned cores. Cores yielding Cenozoic concordant ages display mosaic textures, while young rims show concentric zoning or convoluted zoning (Figure 9A).

5.3. *Interpretation*

Both samples yield three groups of data with distinctive age, chemical, and textural characteristics. The three groups are pre-Cenozoic cores, Cenozoic cores, and Cenozoic rims. The Cenozoic cores and rims mostly have high U/Th ratios, which are commonly associated with metamorphic or hydrothermal events (e.g. Hoskin and Black 2000; Rubatto 2002; Rubatto *et al.* 2006). Both samples have some zircon grains that present mosaic textures in cores and convoluted zoning in rims. Mosaic textures may be developed by metasomatic replacement of zircon or represent metamict or recrystallized zircons (Corfu *et al.* 2003; Rubatto *et al.* 2013), and convoluted zoning may result from late to post-magmatic recrystallization of trace-element-rich domains or later metamorphic events (Corfu *et al.* 2003). Therefore, the chemical and textural characteristics indicate that growth of the zircon grains with Cenozoic ages in both samples is related to metamorphism.

Pre-Cenozoic cores of both samples are interpreted as inheritance, reflecting early Palaeozoic fold-thrust belt development (Gehrels *et al.* 2003, 2006). Cenozoic cores are consistently older than Cenozoic rims for both samples: ages are ca. 34.7–29.4 Ma (cores) and ca. 30.8–23.1 Ma (rims), and ca. 26.7–19.3 Ma (cores) and 18.8–13.8 Ma (rims), for samples DH12-12-10 2 and DH11-21-10 4, respectively. The wide span of Cenozoic ages (ca. 35–13 Ma) from cores to rims indicates protracted zircon growth. This feature has been documented in different Himalayan tectonic domains (e.g. Lee and Whitehouse 2007; Cottle *et al.* 2009; Rubatto *et al.* 2013) and can be interpreted as episodic growth of zircon in the presence of melt if high temperatures were maintained over a long time period (Rubatto *et al.* 2013). Given the chemical and textural distinctions between Cenozoic core and rim ages for both samples, we interpret only the rim ages as leucogranite crystallization ages. Core ages are interpreted as inheritance from earlier metamorphic event(s). Because sample DH12-12-10 2 is of a pre- and/or syn-kinematic intrusion and sample DH11-21-10 4 is of a post-kinematic intrusion within the Galchi shear zone, our interpretation

of Cenozoic rim ages indicates that the Galchi shear zone was active between 23.1 and 18.8 Ma (and possibly earlier) and ceased activity before ca. 18.8–13.8 Ma.

6. Discussion

Field mapping and kinematic analysis along the northern margin of the Kathmandu Nappe confirm that a top-to-the-north shear zone, the Galchi shear zone, separates Sheopuri Gneiss to the north from Bhimphedi Group to the south. In this framework, the Bhimphedi and Phulchauki Groups are the Tethyan Himalayan Sequence as shown by Webb *et al.* (2011a). Quartz *c*-axis fabrics from our westernmost transect across the Galchi shear zone and its hanging wall (1) confirm the top-to-the-north shear kinematics and (2) yield deformation temperatures consistent with observed right-way-up peak metamorphic temperatures (cf. Rai *et al.* 1998; Johnson *et al.* 2001). U-Pb zircon dating of pre-to-syn- and post-kinematic leucogranite demonstrates that the Galchi shear zone was active between 23.1 and 18.8 Ma and ceased activity before ca. 18.8–13.8 Ma. These timing constraints are consistent with our early interpretation of Galchi shear zone activity (Webb *et al.* 2011a) and similarly supported by published U-Pb zircon ages of pre-to-syn-kinematic leucogranite from the westernmost transect across the shear zone (Johnson *et al.* 2001; Webb *et al.* 2011a) and with muscovite cooling ages of ~15–12 Ma across the northern margin of the Kathmandu Nappe (Arita *et al.* 1997; Herman *et al.* 2010). In the following subsections, we discuss the implications of these findings for the emplacement of the Himalayan crystalline core (the Greater Himalayan crystalline complex). We then synthesize the results of the recent literature and this work into a new model for the evolution of the Himalayan orogen, in which duplexing persistently plays the dominant role.

6.1. *The STD at the Kathmandu Nappe*

Webb *et al.* (2011a) initially correlated the Galchi shear zone to the STD on the basis of four criteria: lithological juxtaposition, metamorphic correlations, structural fabrics, and timing of deformation. These criteria are widely applied for recognizing the STD in other regions across the orogen (e.g. Godin *et al.* 2006; Wagner *et al.* 2010; Cottle *et al.* 2011). All these criteria hold true for the four transects investigated in this study across the northern Kathmandu Nappe. Here, we would like to address that the metamorphic sequence across the shear zone plays a key role in making our interpretation. The contrast of metamorphic sequence, i.e. the distinction between right-way-up metamorphic field gradients across the southerly segments of the range *versus* the inverted metamorphic field gradients across the central swaths of the range, is one of the key distinctions in current Himalayan tectonics research. Workers who recognize this distinction (e.g. Leger *et al.* 2013) arrive at starkly different interpretations of orogenic structure to workers who do not recognize it (e.g. Law *et al.* 2013). Thus, the Galchi shear zone is interpreted as the STD along the entire northern margin of the Kathmandu Nappe synform, juxtaposing the Sheopuri Gneiss (i.e. the Greater Himalayan Crystalline complex) to the north with the Bhimphedi Group to the south (Figures 5D and 10). This contact intersects the MCT to the east and west along the northern margin of the Kathmandu Nappe (Stöcklin 1980; Rai *et al.* 1998), so the Galchi shear zone/STD likewise intersects the MCT on the northwest and northeast margin of the nappe (Webb *et al.* 2011a). This geometry requires that the Greater Himalayan Crystalline rocks between the Galchi shear zone/STD and the MCT cut out to the south, representing the frontal tip of this tectonic unit (Figure 6 and 10). Specifically, the thickness of the Greater Himalayan Crystalline complex here decreases southwards (i.e. in the direction of transport), as shown by the five cross sections across the northern Kathmandu Nappe of Figure 10.

One of our major data sets to demonstrate the correlation of the Gachi shear zone and STD is the dominant top-to-the-north shearing in the Gachi shear zone. However, a recent study by Sapkota and Sanislav (2013) shows that both top-to-the-south and top-to-the-north shearing exist in the Kathmandu Nappe by analysing a large number of thin sections. It appears that top-to-the-south shearing dominates the region if indiscriminately looking at all those mixed data together. However, when looking closely at the data from the area of Galchi, we find out that most samples with top-to-the-north shearing are located in an E–W-trending, narrow zone that is coincident with the Galchi shear zone defined by Webb *et al.* (2011a). Outside of this narrow zone characterized by dominance of top-to-the-north shearing, the structural fabrics are overwhelmed by top-to-the-south shearing. Sapkota and Sanislav (2013) propose a hypothesis that the top-to-the-north shearing is a set of youngest (post-MCT) structures in the region representing reactivation of older structural fabrics during folding of the Kathmandu synform. Their model, however, does not consider the first-order structural contact between the Bhimphedi and Sheopuri groups along the northern margin of the Kathmandu Nappe. This contact is mapped in this study as the Galchi shear zone with dominance of top-to-the-north shearing, which was active between 20 and 14 Ma constrained by the U-Pb zircon dating of a deformed leucogranite cutting by top-to-the-north shearing in the Galchi shear zone from the Mahesh Khola transect (Webb *et al.* 2011a) or between 23 and 19 Ma constrained by deformed and undeformed leucogranites in the Galchi shear zone from the Kakani transect and Lapsephedi transect (this study). These ages are much older than the predicted timing of the top-to-the-north shearing in the alternative model of Sapkota and Sanislav (2013). On

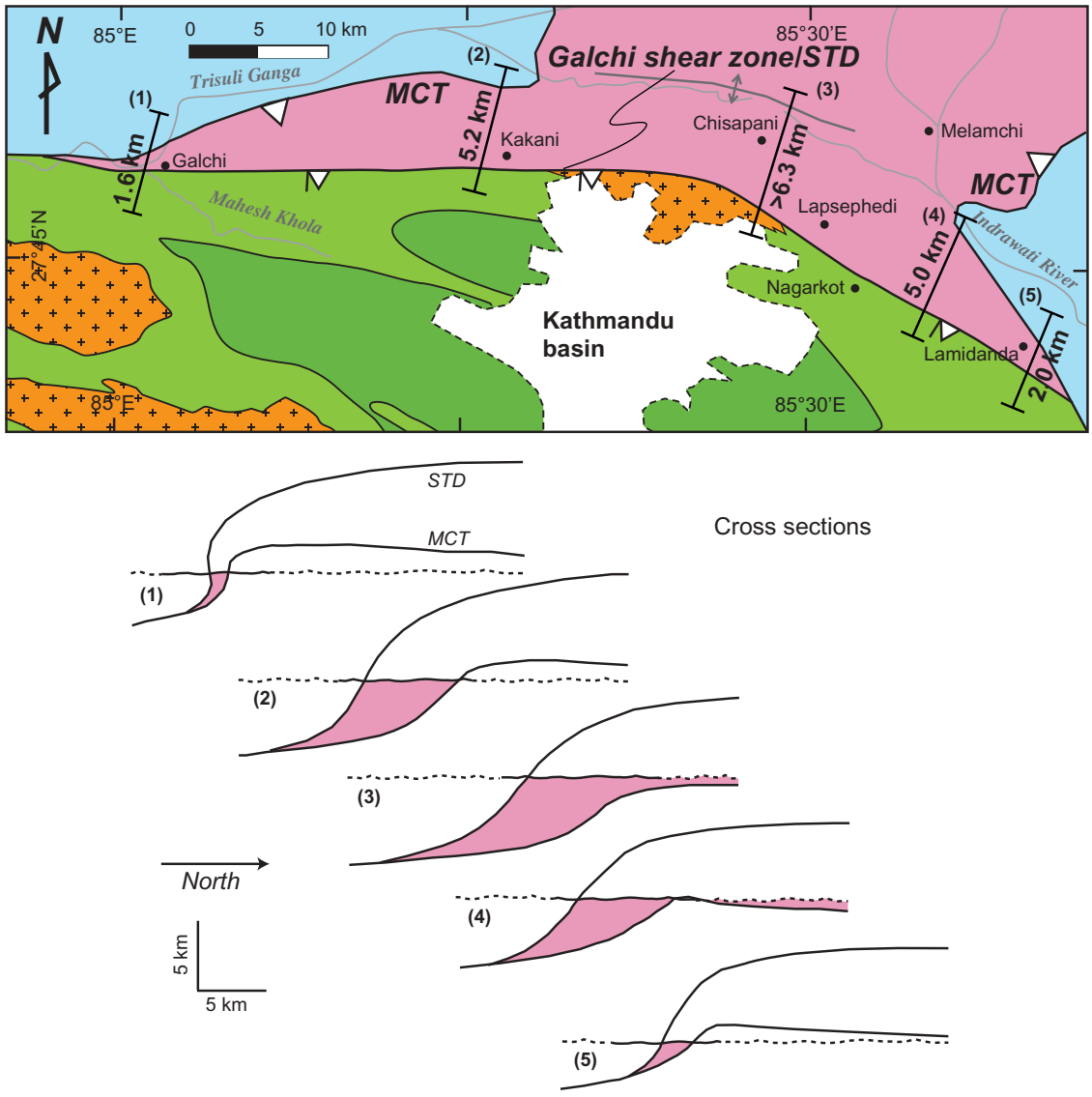

Figure 10. Comparison of five cross sections across the northern margin of the Kathmandu Nappe showing the southward thinning of the Greater Himalayan Crystalline complex in the transport direction.

the other hand, the alternative model is supposed to predict that the top-to-the-north shearing structures are evenly distributed in the northern limb of the Kathmandu synform, but both their data and our data indicate that the top-to-the-north shearing is concentrated in the Galchi shear zone. Therefore, we do not favour this alternative model for interpreting the Galchi shear zone. Nonetheless, some of top-to-the-north shearing structures spotted in the Kathmandu Nappe may be well explained by the model of Sapkota and Sanislav (2013).

6.2. *The horizontal STD*

Although the STD has long been understood as a N-dipping normal fault (or fault zone), there is nonetheless increasingly well-documented evidence that the STD (1) is regionally warped, such that it occurs in a variety of orientations (e.g. Grujic *et al.* 2002; Epard and Steck 2004; Yin 2006; Antolín *et al.* 2013), and (2) was a sub-horizontal shear zone during its early–middle Miocene period of activity (e.g. Yin 2006; Webb *et al.* 2007; Larson *et al.* 2010b). The southward extension of the STD documented in this work, combined with the main trace along the range crest and the likely northern exposures within the Northern Himalayan gneiss domes (Chen *et al.* 1990; Larson *et al.* 2010a; Wagner *et al.* 2010), is consistent with the STD having a broadly sub-horizontal orientation now across ~200 km in the fault transport direction (e.g. Yin 2006; Webb *et al.* 2011a, 2011b; Kellett and Grujic 2012). A sub-horizontal active STD

interpretation is supported by several other lines of evidence: (1) generally consistent exposures of stratigraphic juxtaposition across the STD in the transport direction (e.g. Burchfiel *et al.* 1992; Grujic *et al.* 2002); (2) roughly constant peak P-T conditions across the STD exposures in the transport direction (e.g. Grujic *et al.* 2002; Jessup *et al.* 2008; Kellett *et al.* 2010; Wagner *et al.* 2010); (3) no thermochronological break in the proximal hanging wall and footwall of the STD (e.g. Metcalfe 1993; Godin *et al.* 2001; Vannay *et al.* 2004; Chambers *et al.* 2009; Martin *et al.* 2014); and (4) early–middle Miocene exhumation rates as low as $\ll$0.1 mm/year in STD footwall rocks north of the Kathmandu Nappe (Wobus *et al.* 2008). Therefore, the N-dipping exposures of this fault along the range crest likely were tilted into this orientation by subsequent deformation (Yin *et al.* 2010; Long *et al.* 2011; Webb 2013; McQuarrie *et al.* 2014).

With reference to the first line of evidence cited earlier, it is worth noting that the STD does not uniformly maintain the same hanging wall stratigraphy across the breadth and width of the Himalaya. For example, if the common interpretation that many North Himalayan gneiss domes are bounded by the STD is correct (e.g. Chen *et al.* 1990; Larson *et al.* 2010a; Wagner *et al.* 2010), then the STD hanging wall protolith lithologies in many such positions are significantly younger than elsewhere in the orogen. This could be interpreted to indicate N-directed thrusting, but may just as readily reflect regional stratigraphic variations. Similar variations commonly show large swaths of 'missing section' in low-deformation portions of the orogen (e.g. Vannay and Steck 1995). Such a section is missing via unconformities, not faults (e.g. Frank *et al.* 1995; Vannay and Steck 1995), so subsequent cutting by a flat fault would coincide with changes in stratigraphy.

A final component of evidence that is commonly cited to support a N-dipping normal fault STD is local juxtaposition of high-grade Greater Himalayan Crystalline complex rocks with low-grade Tethyan Himalayan Sequence rocks along steeply N-dipping brittle normal faults. Such relationships occur because some normal faults with generally less than 5 km of displacement were active late in the deformation history (e.g. Epard and Steck 2004; Webb *et al.* 2013; Robyr *et al.* 2014). Examples include the Sarchu Normal fault of northwest India and normal faults along the Bhutan–southeast Tibet border (e.g. Steck *et al.* 1993; Edwards *et al.* 1996). These faults locally excise some or the entire STD shear zone, and because flattening within the STD shear zone produced an apparent compressed geothermal gradient (e.g. Law *et al.* 2011), the apparent thermal offset across these small normal faults can seem profound. Nonetheless, these are minor features with small offsets that postdate STD shearing (Epard and Steck 2004; Webb *et al.* 2013; Robyr *et al.* 2014).

6.3. *The MCT-STD branch line along the Himalayan arc*

With the preceding clarification of the sub-horizontal geometry of the STD during slip, and the results of this study showing the southern extension of the STD and the frontal tip of the Greater Himalayan Crystalline complex along the northern Kathmandu Nappe, we now proceed to assess the universality of the MCT-STD branch line along the southern reaches of the orogen (Figure 3). To the west of the Kathmandu Nappe, numerous works have documented this relationship in recent years. Yin's (2006) synthesis suggested the presence of the MCT-STD branch line in the Zanskar and Himachal regions of northwest India; Webb *et al.* (2007, 2011b) used integrated tectonic investigations to confirm the essentials of this relationship in Himachal (Figure 1). Webb *et al.* (2011a) proposed the occurrence of the MCT–STD branch line in the Dadeldhura Klippe of western Nepal; both Antolín *et al.* (2013) and He *et al.* (2014) confirm the southern extension of the STD along the northern margin of the klippe and show that the STD and MCT occur within ~1 km of each other. He *et al.* (2014) further demonstrate that the Greater Himalayan Crystalline complex thins from north to south in the Dadeldhura region. Therefore, unless the faults diverge farther south as shown by Antolín *et al.* (2013), the MCT–STD branch line must occur there as well. In the Annapurna–Dhaulagiri region of Nepal, the MCT and STD lie closely together: the crystalline rocks between the two shear zones are only ~2–6 km thick (Hodges *et al.* 1996; Vannay and Hodges 1996; Searle and Godin 2003; Godin *et al.* 2006; Larson and Godin 2009; Carosi *et al.* 2007, 2010; Martin *et al.* 2014) but do not intersect each other. In this region, the MCT–STD branch line is interpreted to be eroded away (Figure 4). For most other regions west of Kathmandu, the branch line also appears to be eroded away. If the MCT–STD branch line is an orogen-wide feature, the along-strike thickness variation of the crystalline rocks (e.g. ~20 km in eastern Nepal vs. ~2–6 km in central and western Nepal) can be interpreted to reflect across-strike thinning of the crystalline rocks (Figures 3 and 4). Specifically, regions with thick crystalline rocks indicate that the exposures represent the rear (hinterland) part of the crystalline core while regions with thin crystalline rocks indicate that the exposures are the front (foreland) part of the crystalline core.

This study demonstrates that the boundary between the Greater Himalayan Crystalline complex (i.e. the Sheopuri Gneiss) and the Bhimphedi Group in the Kathmandu Nappe is characterized by the southern extension of the STD. Lombardo *et al.* (1993) show the Sheopuri–Bhimphedi contact extending to the southern portion of eastern Nepal, where the contact is interpreted as a S-dipping, N-directed thrust fault. Based on the criteria presented here, we also interpret this contact in eastern Nepal as a southern extension of the STD and its

intersection with the MCT as the MCT–STD branch line (Figures 1 and 3). Similar outcroppings of the branch line may exist farther east, from southeastern Nepal as far as southeastern Bhutan (following and locally re-interpreted from Lombardo *et al.* 1993; Goscombe and Hand 2000; Grujic *et al.* 2002; Long and McQuarrie 2010; Long *et al.* 2011). Farther east in the Arunachal Himalaya (India), the branch line appears to be eroded away (Figure 1).

The orogen-wide distribution of the MCT-STD branch line indicates that focused erosion may not play a crucial role in the emplacement of the crystalline core, although precipitation and erosion have played a major role in shaping the orogenic evolution. Specifically, focused erosion is not a main driver to suck the crystalline core to the surface (cf., Beaumont *et al.* 2001), because the leading edge of the crystalline core is preserved in many regions across the orogen. Many recent studies also suggest that there is no simple relationship between precipitation, erosion, and structural evolution in the orogen (e.g. Burbank *et al.* 2003; cf., Wobus *et al.* 2005; Bookhagen and Burbank 2006; Blythe *et al.* 2007; Thiede *et al.* 2009; Thiede and Ehlers 2013).

In summary, the southern trace of the STD merges with the MCT in several regions of the southern Himalaya. The widespread distribution of the MCT–STD branch line along the length of the range indicates that it is an orogenic feature rather than a local anomaly (Figure 1). In the following subsections, we review the consequences of this geometry for Himalayan kinematic models.

6.4. *Emplacement of the Himalayan crystalline core*

The range of kinematic models proposed for the emplacement of the Himalayan crystalline core – wedge extrusion, channel flow, tectonic wedging, and duplexing – are presented schematically in Figure 2. These schematic representations capture the most common versions of each model. Models labelled 'critical taper' are also commonly promoted, but the general kinematics of these typically match the wedge extrusion model, or in some cases the duplexing model. The features documented by this work, i.e. the southwards MCT–STD merger and the present-day local burial of the frontal tip of the Greater Himalayan Crystalline complex, are only consistent with the tectonic wedging model (Figure 2C) (or the early tunnelling stage of the channel flow model, which shares similar kinematics to tectonic wedging, without a significant late focused denudation and exhumation stage). The other kinematic models show the Greater Himalayan Crystalline complex exhumed to the surface by the early to middle Miocene, but such a scenario is impossible to square with current preservation of the leading edge of this unit. Given such exhumation, the leading edge rocks would all be eroded away by now.

Other models offer important perspectives on the emplacement of the Himalayan crystalline core. First, channel flow models offer a compelling focus and range of predictions concerning internal kinematics of the crystalline rocks, and the latest channel flow models are consistent with known geometries. As the evidence for a southwards MCT–STD merger and the present-day local burial of the frontal tip of the Greater Himalayan Crystalline complex mounts (e.g. Yin 2006; Webb *et al.* 2007, 2011a, 2011b; Leger *et al.* 2013; He *et al.* 2014; this work), workers exploring the potential importance of southwards tunnelling of channelized lower/middle crust are gradually modifying the kinematics of the channel flow model. The late exhumation stage is de-emphasized or discarded, and the tunnelling stage expanded into younger periods (e.g. Larson *et al.* 2010b; Kellett and Grujic 2012; Larson and Cottle 2014), such that many recent implementations of channel flow models share first-order kinematics with tectonic wedging models. Convergence of kinematic models is a promising development. Second, duplexing models are most commonly represented as shown with the Greater Himalayan Crystalline complex exhumed to the surface in the early to middle Miocene (e.g. Carosi *et al.* 2010; Imayama *et al.* 2012; Mukherjee *et al.* 2012; Montomoli *et al.* 2013). However, recent tectonic wedging modelling has involved some duplexing (Webb *et al.* 2013), or duplexing models have involved some channel tunnelling/tectonic wedging (Larson and Cottle 2014), such that the concept is the same: the STD is envisioned as the roof thrust to a duplex made of Greater Himalayan Crystalline complex horses for at least a period of Himalayan shortening.

6.5. *Internal development of the Himalayan crystalline core*

Here, we explore the internal kinematics of the Greater Himalayan Crystalline complex and corresponding implications for orogenic mechanics.

6.5.1. *Key findings: discontinuities, flattening, and melting*

Recent suggestions that duplexing may dominate much of the assembly of the Greater Himalayan Crystalline complex are based on the recognition of multiple faults within the Greater Himalayan Crystalline complex across the entire Nepal Himalaya (Figure 3; e.g. Reddy *et al.* 1993; Carosi *et al.* 2010; Martin *et al.* 2010; Corrie and Kohn 2011; Imayama *et al.* 2012; Wang *et al.* 2013; Larson and Cottle 2014). These faults are parallel to the MCT, feature top-to-the-south thrusting, and generally show younger periods of motion at lower structural positions. This in-sequence structural development is not entirely uniform: Rubatto *et al.* (2013) documented a reversal of this pattern

at the upper structural levels of the Greater Himalayan Crystalline complex in the Sikkim Himalaya, and an out-of-sequence structures are recognized elsewhere (e.g. Larson and Cottle 2014; Warren *et al.* 2014). The general pattern appears consistent with the recent hypothesis that the Greater Himalayan Crystalline complex is not a uniform unit or fossilized distributed flow channel but rather consists of multiple slices that have been assembled since the Oligocene via dominant duplexing and minor out-of-sequence faulting (Martin *et al.* 2010; Corrie and Kohn 2011; Montomoli *et al.* 2013; Webb *et al.* 2013; Larson and Cottle 2014), a process similar to the development of the Lesser Himalayan Sequence duplex (e.g. Robinson *et al.* 2003; Konstantinovskaia and Malavieille 2005; Herman *et al.* 2010; Martin *et al.* 2010; Long *et al.* 2011; Webb 2013).

Another key feature that informs our understanding of Himalayan crystalline core development is the pervasive development of foliation and corresponding foliation-perpendicular flattening strain (e.g. Vannay and Grasemann 2001; Carosi *et al.* 2006; Corrie *et al.* 2012). This flattening is commonly understood to represent deformation/flow at depth within the orogenic wedge, perhaps within a channel (e.g. Beaumont *et al.* 2004; Larson *et al.* 2010b). However, Long *et al.* (2011) presented a model for the development of foliation in Lesser Himalayan thrust sheets suggesting that these fabrics develop during burial *below* the orogenic wedge, prior to accretion of thrust sheets from the downgoing plate and synchronously with peak metamorphism. These authors allow that the same process may occur during development of the Greater Himalayan Crystalline complex.

Work on the channel flow model has focused attention on the ability of melts to substantially lower viscosities of rock packages and thus allow zones of enhanced flow (e.g. Nelson *et al.* 1996; Beaumont *et al.* 2001). Because most exposed Cenozoic Himalayan igneous rocks are leucogranites produced by dehydration melting of metapelites (Patino Douce and Harris 1998), these melts may have been generated by decompression and/or heating (strain heating or burial heating). Heating could occur prior to accretion in the downgoing Indian plate, whereas decompression melting can occur only after initiation of exhumation. Exploration of potential kinematic consequences has largely focused on melting within the orogenic wedge, where it may permit rapid sub-horizontal and/or sub-vertical motion (e.g. Beaumont *et al.* 2001; Faccenda *et al.* 2008).

A key recent breakthrough in understanding the kinematics of the partially molten rocks is the discovery of correlations between the timing of melting and structural position. Pressure–temperature–time evolutions associated with partially molten rocks commonly show 5−10 million year periods encompassing prograde metamorphism, melting, and initial rapid cooling, and the absolute age of each period correlates with the positions of tectonic discontinuities within the Greater Himalayan Crystalline complex (Corrie and Kohn 2011; Montomoli *et al.* 2013; Rubatto *et al.* 2013; Larson and Cottle 2014). For example, Corrie and Kohn (2011) reported in Central Nepal three thrust slices (Sinuwa thrust sheet, Bhanuwa thrust sheet, and MCT thrust sheet) with similar prograde through exhumation P-T-t patterns spanning 27–23, 23–19, and 19–15 Ma (younging from north to south). In many cases, the age of each period is progressively younger in structurally lower thrust sheets (unless the pattern is disrupted by late out-of-sequence faults, as in parts of the eastern Himalaya: Grujic *et al.* 2011; Warren *et al.* 2011, 2014; Regis *et al.* 2014). Therefore, the melting process may be correlated with the deformation pathway experienced by each thrust sheet; the thrusts may not reflect disruption of an emplaced, previously partially molten channel. Restating this distinction, consider that the oldest melts of a channel would be farthest south (Nelson *et al.* 1996), so if thrust stacking post-dates melting the oldest melts should be at the base of the southward-propagating duplex. In contrast, melting during decompression following accretion of each successive thrust sheet would produce southwards younging of melting and cooling periods (e.g. Corrie and Kohn 2011; Rubatto *et al.* 2013). In this model context, we can limit the role of melting-induced deformation, because it does not appear to have disrupted the overall duplex geometry of the Greater Himalayan Crystalline complex, as represented by the tectonic discontinuities.

6.5.2. *The missing components of channel flow*

Montomoli *et al.* (2013) argued that the imbrication inherent in Greater Himalayan Crystalline complex duplexing limits the maximum thickness of any one slab of the unit to less than a 20–30 km thickness necessary for channel flow. In short, they argue that channel flow models may be running out of room (cf. Grujic 2006). Here we broaden this view: the channel flow models, including models involving only channel tunnelling with no late focused exhumation phase, may be running out of *components*.

As reviewed by Beaumont *et al.* (2001), the channel flow model calls for (1) partially molten crust and (2) concentrated rapid denudation to explain contemporaneous (3) MCT shortening and (4) STD motion (which can be subdivided into a tunnelling period followed by extension), (5) the development of gneiss domes in south Tibet, and differences between the Greater Himalayan Crystalline complex and Lesser Himalayan Sequence in terms of (6) protoliths and (7) P-T-t paths. For the first component, (1) partially molten crust, the immediately preceding section outlines that melts did not traverse tectonic discontinuities within the Greater Himalayan Crystalline complex. Concentrated rapid denudation, point (2), is limited by (i) the preservation of the leading

edge of the Greater Himalayan Crystalline complex, as documented in this work (and elsewhere: Yin 2006; Webb *et al.* 2007, 2011a, 2011b), and (ii) the very low exhumation rate (e.g. ≪0.1 mm/year in north of Kathmandu Nappe by Wobus *et al.* 2008; ~0.6 mm/year in NW Himalaya by Thiede *et al.* 2009; ~0.5 mm/year in central Nepal and 0.2–1.2 mm/year for the Sutlej region by Thiede and Ehlers 2013) of the Greater Himalayan Crystalline complex rocks in the early–middle Miocene as compared to the exhumation rates (1–3 mm/year) of the same rocks from the late Miocene to present. The MCT–STD branch line described here precludes extension along the STD, so within the channel flow kinematic context, only tunnelling can be considered for contemporaneous MCT, point (3), and STD motion, point (4). Without consideration of internal Greater Himalayan Crystalline complex kinematics and a late phase of STD extension, tunnelling kinematics may be identical to tectonic wedging kinematics. Considering internal kinematics, melting and accompanying decreases in viscosity could permit outwards flow forced by the high gravitational potential of the Tibetan Plateau, but as discussed earlier, such flow appears limited to the scale of individual tectonic discontinuities within the Greater Himalayan Crystalline complex. Many Himalayan gneiss domes, point (5), display arc-parallel extension, which reflects partitioning of 3D strain that is largely independent of (and of small magnitude relative to) arc-perpendicular shortening (Styron *et al.* 2011). Domes that display only arc-perpendicular transport may also develop by accretion and duplexing/antiformal stacking beneath the fold of the dome (Yin 2004). Channels are not necessary, and associated upwards flow for gneiss dome development does not appear likely given the increasing recognition of single-folded shear zones bounding the upper limits of many Himalayan gneiss domes (e.g. Larson *et al.* 2010a; Wagner *et al.* 2010). Protolith differences, point (6), of Greater and Lesser Himalayan rocks do not allow model testing: a variety of possible pre-deformation stratigraphic configurations, plus thrust fault slips that commonly are of sufficient magnitude to obscure cut-off relationships via footwall burial and/or hanging wall erosion, permit a wide range of deformation models. Finally, as discussed earlier, the P-T-t paths of Greater and Lesser Himalayan rocks, point (7), appear to have more in common than previously thought, since both can be achieved via burial and accretion of thrust slices (Herman *et al.* 2010; Corrie and Kohn 2011; Long *et al.* 2011). The stacking of Greater Himalayan slices with similar P-T-duration loops at different absolute ages is not consistent with a simple channel flow (Corrie and Kohn 2011; Montomoli *et al.* 2013; Rubatto *et al.* 2013). As discussed earlier, flattening strain has also been considered representative of channel flow (e.g. Larson *et al.* 2010b), but may be consistent with deformation prior to accretion (Long *et al.* 2011). In summary, every component of the channel flow model is either precluded by evidence collected over the last 10 years (points (2)–(4), (7)), or may be explained by an alternative process (points (1), (3)–(7), *flattening*).

6.5.3. *Mechanics: channel flow vs. critical taper, or a different dichotomy? or What's the most useful dichotomy?*

Discussions of the mechanics of Himalayan crystalline core development and emplacement commonly centre on two models: channel flow and critical taper (e.g. Beaumont *et al.* 2004; Kohn 2008; Larson *et al.* 2010b; Robinson and Pearson 2013). In contrast to the forcing via gravitational potential and focused erosion that drives extrusion of a zone of melt-weakened rock in the channel flow model (Beaumont *et al.* 2001), the critical taper model allows the orogenic wedge to fail internally at any location(s) in order to maintain a critical wedge slope that reflects a balance of compressional and resisting forces (Davis *et al.* 1983). Many workers have advocated that channel flow *versus* critical taper is a false dichotomy, because the two tectonic styles may coexist and overlap in nature. Channel flow mechanics may dominate in the hinterland, critical taper may control foreland deformation, and the boundary between the two zones may shift over time (Larson *et al.* 2010b, 2013; Corrie *et al.* 2012; Jamieson and Beaumont 2013; Larson and Cottle 2014). At least in terms of kinematic distinctions, we agree that this is a false dichotomy. Both channel flow and critical taper models require extensive deformation of the upper plate to explain key aspects of the tectonic development of the Greater and Tethyan Himalayan rocks, most importantly slip on the South Tibet detachment and Great Counter thrust.

We argue that a more useful dichotomy with which to frame exploration of the internal development of the Greater Himalayan Crystalline complex is the distinction of upper plate deformation models (e.g. Beaumont *et al.* 2001; Jamieson *et al.* 2004; Godin *et al.* 2006; Harris 2007) *versus* accretionary models in which the dominant formation process is accretion to the upper plate of horses derived from downgoing Indian crust (e.g. Robinson *et al.* 2003; Bollinger *et al.* 2004, 2006; Herman *et al.* 2010). In short, the important dichotomy is extrusion solely in the upper plate *versus* duplexing by accretion from the lower plate. Significant deformations that must occur in the upper plate are (1) flow related to melt weakening, (2) N-directed backthrusting along the STD (e.g. this work, Yin 2006), (3) slip on the Great Counter thrust (likely linked to the STD, e.g. Yin *et al.* 1999), (4) S-directed out-of-sequence thrusting (e.g. Larson and Cottle 2014), and (5) folding in response to development of underlying duplexes and antiformal stacks. Flow of partially molten rock does not appear to have disrupted faults within the Greater Himalayan Crystalline complex and is

correspondingly limited in magnitude. Backthrusting and out-of-sequence thrusting may accomplish significant shortening that nonetheless would be modest in comparison to the slip along the basal thrust system. Sub-parallel tectonic discontinuities within the Greater Himalayan Crystalline complex suggest only minor folding due to accretion during development of this unit. Folding subsequent to MCT and STD motion is an under-appreciated control on the present-day geometry of these structures, particularly the STD (Schelling and Arita 1991; Schelling 1992; Thakur and Rawat 1992; Srivastava and Mitra 1994; Yin 2006; cf. Law *et al.* 2011). Combined, these limits on upper plate processes during Greater Himalayan Crystalline complex development suggest the dominance of accretion and duplex development.

6.6. *Duplexing dominates Himalayan orogenesis*

In this work, we discuss how some key components of extrusion models for development of the Greater Himalayan Crystalline complex are precluded by geometric and kinematic evidence, and the rest can be explained via underplating and duplex development. Growth of the Tethyan Himalayan Sequence fold-thrust belt is widely acknowledged to result from forward propagation of thrusting, forming an imbricate fan (e.g. McElroy *et al.* 1990; Steck *et al.* 1993; Ratschbacher *et al.* 1994; Frank *et al.* 1995; Fuchs and Linner 1995; Searle *et al.* 1997; Wiesmayr and Grasemann 2002; Murphy and Yin 2003). Duplexing is recognized as the dominant process that assembled the Lesser Himalayan Sequence since the late Miocene, with out-of-sequence deformation restricted to $\ll$10% of shortening (e.g. DeCelles *et al.* 2001; Robinson *et al.* 2003; Bollinger *et al.* 2004, 2006; Herman *et al.* 2010; Webb 2013; McQuarrie *et al.* 2014). Recent seismic and interferometric synthetic aperture radar experiments reveal that duplexing may still continue at multiple crustal levels at present (Nábělek *et al.* 2009; Grandin *et al.* 2012). Taken together, Himalayan mountain building appears to record thrust stacking almost exclusively with dominance of duplexing processes since the early development of the Greater Himalayan Crystalline complex.

By synthesizing these findings, an evolutionary history of the central Himalaya after the initial Indian–Asian collision is proposed (Figure 11). The first stage we represent is the post-collisional crustal thickening via accretion of the Tethyan Himalayan Sequence. These rocks experienced intense south-verging, isoclinal folding, and south-

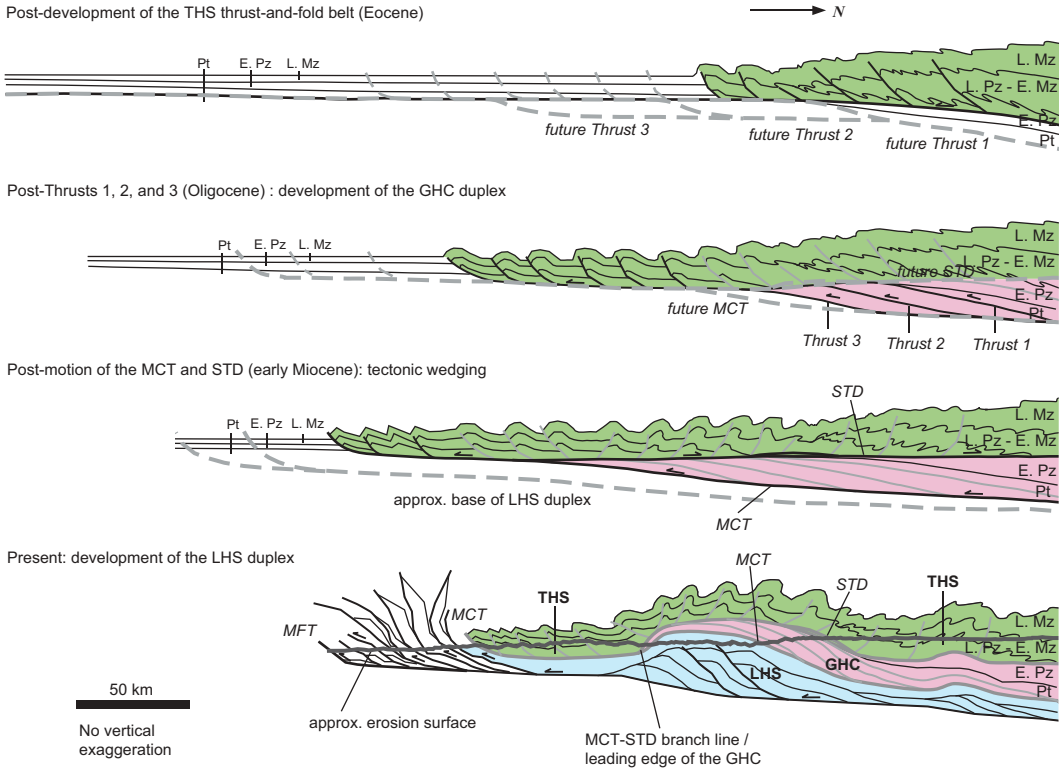

Figure 11. Schematic cross sections showing Cenozoic evolution of the central Himalaya after India–Asia collision. Abbreviations and colour codes as in Figure 2. Dashed lines mark future faults; black bold lines are active faults; grey bold lines are inactive faults. The deeper duplex developed in the Lesser Himalaya Sequence (bottom figure) is a model for the formation of the Northern Himalayan Gneiss domes proposed by Murphy (2007), and a presently active underplating process at this position is supported by the Hi-CLIMB experiment (Nábělek *et al.* 2009). See text for details.

directed thrusting after the initial Indian–Asian collision (e.g. Ratschbacher *et al.* 1994; Godin *et al.* 1999, 2001; Yin *et al.* 1999; Wiesmayr and Grasemann 2002; Murphy and Yin 2003; Aikman *et al.* 2008; Kellett and Godin 2009; Searle 2010). Development of the Tethyan Himalayan Sequence fold-thrust belt via accretion likely continued in the foreland during initial metamorphism and accretion of Greater Himalayan Crystalline complex horses in the hinterland (Carosi *et al.* 2010; Corrie and Kohn 2011). To provide a conceptual framework, we use the names Thrust 1, Thrust 2, and Thrust 3 to label three S-directed thrust faults within the Greater Himalayan Crystalline complex here; they are examples and generalized from three thrusts introduced in the western and central Nepalese Himalaya by Carosi *et al.* (2010) and Corrie and Kohn (2011): the Sinuwa thrust, Toijem shear zone, and Bhanuwa thrust. These three internal thrust faults have been interpreted as being active at 27, 26, and 23 Ma, respectively, although the ages of the Sinuwa thrust and Toijem shear zone may not be distinguishable when considering the measuring errors. Nonetheless, the development of duplex within the Greater Himalayan Crystalline complex via internal thrusting has been documented by many studies (e.g. Reddy *et al.* 1993; Corrie and Kohn 2011; Wang *et al.* 2013; Webb *et al.* 2013; Larson and Cottle 2014). Shortening accommodated by these three thrust faults is up to 200 km, which has not been included in balanced shortening estimates (e.g. Webb 2013; McQuarrie *et al.* 2014).

The backthrusting, sub-horizontal STD may have acted as a roof thrust to the accumulating Greater Himalayan Crystalline complex below (à la Dunne and Ferrill 1988; Erickson 1995; Jones 1996). Such kinematics would combine elements of the duplexing and tectonic wedging models (Figure 12). After the early–middle Miocene, motion along the MCT and STD ceased, and the Lesser Himalayan Sequence duplex in the MCT footwall began to develop (Herman *et al.* 2010). This duplexing warped the MCT, STD, and the rocks above both thrusts (e.g. Robinson *et al.* 2003; McQuarrie *et al.* 2008; Webb *et al.* 2013). The leading edge of the Greater Himalayan Crystalline complex is still locally preserved in places such as the Kathmandu Nappe (this study) and Dadeldhura klippe (He *et al.* 2014), but it has been eroded away in many other parts of the orogen. Duplexing continues to act as the main growth and deformation mechanism of ongoing orogenesis at depth (Nábělek *et al.* 2009; Grandin *et al.* 2012).

7. Conclusions

This represents the third and final paper in a series exploring the roles of extrusion *versus* duplexing processes in Himalayan mountain building. The first paper (Yu *et al.* 2014) sufficiently resolves outstanding questions of structural geometry in the northwestern Indian Lesser Himalayan Sequence to demonstrate that duplexing dominates middle Miocene to recent mountain building in that region. The second paper (He *et al.* 2014) demonstrates the southwards convergence of the MCT and STD along the Dadeldhura klippe of western Nepal via evidence of progressively thinning of the Greater Himalayan Crystalline complex from north to south and elucidates the basic function of the STD as a backthrust, not a normal fault. In the current article, the integration of field mapping, kinematic analysis, and U-Pb zircon dating confirms the interpretation that the mainly top-to-the-north Galchi shear zone exists across the entire northern Kathmandu Nappe. The Galchi shear zone is the southern continuation of the STD and merges with the MCT at depth southwards. This work provides additional field evidence that the MCT–STD branch line exists in the Himalayan orogen (e.g. Yin 2006; Webb *et al.* 2007, 2011a, 2011b; Leger *et al.* 2013; He *et al.* 2014). The MCT–STD branch line is

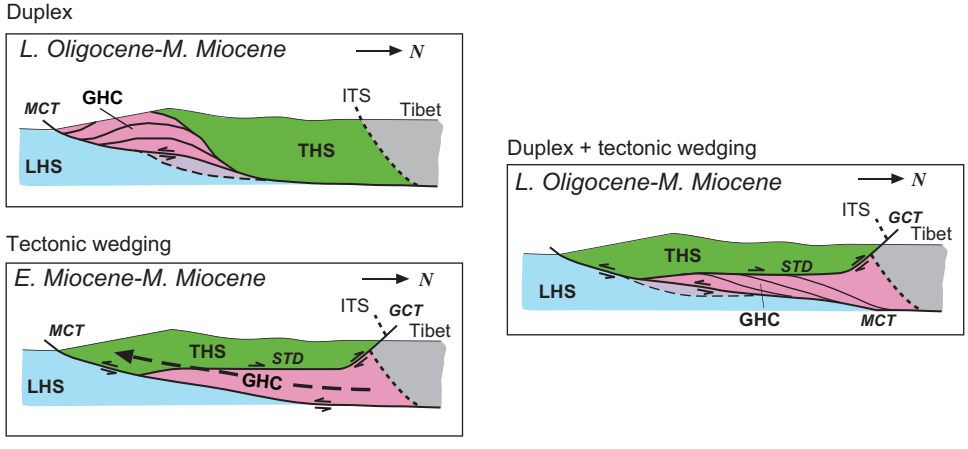

Figure 12. A kinematic model integrating duplexing and tectonic wedging showing the evolution of the Greater Himalayan Crystalline complex.

an orogen-wide feature and serves as a key criterion to distinguish extrusion *versus* duplexing models. These findings, combined with other recent work (Martin *et al.* 2010; Corrie and Kohn 2011; Montomoli *et al.* 2013; Larson and Cottle 2014; Yu *et al.* 2014), are synthesized in a reconstruction showing that Himalayan mountain building since initial Indian–Asian collision has been dominated by accretion and duplexing processes at depth.

Acknowledgements

Discussions with Clayton Campbell, Peter Clift, Cindy Colón, Dennis Donaldson, An Li, Nadine McQuarrie, Eric Weigand, and Hongjiao Yu helped to clarify concepts in this manuscript. We thank R. Carosi and D. Robinson for their constructive reviews and R. Stern for his editorial handling. We thank Bhim Chand and his colleagues at Earth's Paradise Treks and Adventures for field logistical support.

Funding

This work was supported by a GSA student research grant to Dian He and grants from Louisiana State University (start-up), the Louisiana Board of Regents (LEQSF 702 (2012-15)-RD-A-12), and the Tectonics program of the U.S. National Science Foundation (EAR-1322033).

Supplemental data

Supplemental data for this article can be accessed at http://dx.doi.org/10.1080/00206814.2014.986669.

References

Adams, B.A., Hodges, K.V., Van Soest, M.C., and Whipple, K. X., 2013, Evidence for pliocene-quaternary normal faulting in the hinterland of the Bhutan Himalaya: Lithosphere, v. 5, p. 438–449. doi:10.1130/L277.1

Aikman, A.B., Harrison, T.M., and Lin, D., 2008, Evidence for early (>44 Ma) Himalayan crustal thickening, Tethyan Himalaya, southeastern Tibet: Earth and Planetary Science Letters, v. 274, p. 14–23. doi:10.1016/j.epsl.2008.06.038

Allmendinger, R.W., 2012, Stereonet 7.2.4, http://www.geo.cornell.edu/geology/faculty/RWA/programs/stereonet.html (accessed March 2012).

Antolín, B., Godin, L., Wemmer, K., and Nagy, C., 2013, Kinematics of the Dadeldhura klippe shear zones (W Nepal): Implications for the foreland evolution of the Himalayan metamorphic core: Terra Nova, v. 25, p. 282–291.

Arita, K., 1983, Origin of the inverted metamorphism of the Lower Himalayas Central Nepal: Tectonophysics, v. 95, p. 43–60. doi:10.1016/0040-1951(83)90258-5

Arita, K., Dallmeyer, R.D., and Takasu, A., 1997, Tectonothermal evolution of the Lesser Himalaya, Nepal: Constraints from 40Ar/39Ar ages from the Kathmandu Nappe: The Island Arc, v. 6, p. 372–385. doi:10.1111/j.1440-1738.1997.tb00047.x

Avouac, J.-P., 2007, Dynamic processes in extensional and compressional settings-mountain building: From earthquakes to geological deformation, *in* Watts, A.B., ed., Treatise of geophysics, crust and lithosphere dynamics, Volume 6: Boston, Massachusetts, Elsevier, p. 377–439. doi:10.1016/B978-044452748-6.00112-7

Beaumont, C., Jamieson, R.A., Nguyen, M.H., and Lee, B., 2001, Himalayan tectonics explained by extrusion of a low-viscosity crustal channel coupled to focused surface denudation: Nature, v. 414, p. 738–742. doi:10.1038/414738a

Beaumont, C., Jamieson, R.A., Nguyen, M.H., and Medvedev, S., 2004, Crustal channel flows: 1. Numerical models with applications to the tectonics of the Himalayan-Tibetan orogen: Journal of Geophysical Research, v. 109, p. B06406. doi:10.1029/2003JB002809.

Beyssac, O., Bollinger, L., Avouac, J.-P., and Goffé, B., 2004, Thermal metamorphism in the lesser Himalaya of Nepal determined from Raman spectroscopy of carbonaceous material: Earth and Planetary Science Letters, v. 225, p. 233–241. doi:10.1016/j.epsl.2004.05.023

Bhattacharyya, K., and Mitra, G., 2009, A new kinematic evolutionary model for the growth of a duplex – An example from the Rangit duplex, Sikkim Himalaya, India: Gondwana Research, v. 16, p. 697–715. doi:10.1016/j.gr.2009.07.006

Bilham, R., Larson, K., Freymuller, J., and Members, P.I., 1997, GPS measurements of present day convergence across the Nepal Himalaya: Nature, v. 386, p. 61–64. doi:10.1038/386061a0

Blythe, A.E., Burbank, D.W., Carter, A., Schmidt, K.M., and Putkonen, J., 2007, Plio-quaternary exhumation history of the central Nepalese Himalaya: 1. Apatite and zircon fission track and apatite (U-Th)/He analyses: Tectonics, v. 26, p. TC3002. doi:10.1029/2006TC001990.

Bollinger, L., Avouac, J.P., Beyssac, O., Catlos, E.J., Harrison, T. M., Grove, M., Goffé, B., and Sapkota, S., 2004, Thermal structure and exhumation history of the Lesser Himalaya in central Nepal: Tectonics, v. 23. doi:10.1029/2003TC001564.

Bollinger, L., Henry, P., and Avouac, J.P., 2006, Mountain building in the Nepal Himalaya: Thermal and kinematic model: Earth and Planetary Science Letters, v. 244, p. 58–71. doi:10.1016/j.epsl.2006.01.045

Bookhagen, B., and Burbank, D.W., 2006, Topography, relief, and TRMM-derived rainfall variations along the Himalaya: Geophysical Research Letters, v. 33. doi:10.1029/2006GL026037.

Brunel, M., 1986, Ductile thrusting in the Himalayas: Shear sense criteria and stretching lineations: Tectonics, v. 5, p. 247–265. doi:10.1029/TC005i002p00247

Burbank, D.W., Blythe, A.E., Putkonen, J., Pratt-Sitaula, B., Gabet, E., Oskin, M., Barros, A., and Ojha, T.P., 2003, Decoupling of erosion and precipitation in the Himalayas: Nature, v. 426, p. 652–655. doi:10.1038/nature02187

Burchfiel, B.C., Chen, Z., Hodges, K.V., Liu, Y., Royden, L.H., Deng, C., and Xu, J., 1992, The South Tibetan detachment system, Himalaya orogen: Extension contemporaneous with and parallel to shortening in a collisional mountain belt: Geological Society of America Special Paper, v. 269, p. 41.

Burchfiel, B.C., and Royden, L.H., 1985, North-south extension within the convergent Himalayan region: Geology, v. 13, p. 679–682. doi:10.1130/0091-7613(1985)13<679:NEWTCH>2.0.CO;2

Burg, J.P., Brunel, M., Gapais, D., Chen, G.M., and Liu, G.H., 1984, Deformation of leucogranites of the crystalline main central sheet in southern Tibet (China): Journal of Structural Geology, v. 6, p. 535–542. doi:10.1016/0191-8141(84)90063-4

Caby, R.P., and Le Fort, P., 1983, Le grand chevauchement central himalayen: Nouvelles données sur le métamorphisme inverse

à la base de la Dalle du Tibet: Reviews Geological Dynamics Géogr Physical, v. 24, p. 89–100.

Carosi, R., Montomoli, C., Rubatto, D., and Visonà, D., 2010, Late oligocene high-temperature shear zones in the core of the Higher Himalayan Crystallines (Lower Dolpo, western Nepal): Tectonics, v. 29, p. TC4029. doi:10.1029/2008TC002400.

Carosi, R., Montomoli, C., and Visona, D., 2006, Normal-sense shear zones in the core of Higher Himalayan Crystallines (Bhutan Himalaya): Evidence for extrusion? *in* Law, R.D., Searle, M.P., and Godin, L., eds., Channel flow, ductile extrusion and exhumation in continental collision zones: Geological Society, London, Special Publication 268, p. 425–444.

Carosi, R., Montomoli, C., and Visonà, D., 2007, A structural transect in the Lower Dolpo: Insights on the tectonic evolution of Western Nepal: Journal of Asian Earth Sciences, v. 29, p. 407–423. doi:10.1016/j.jseaes.2006.05.001

Catlos, E.J., Dubey, C.S., Harrison, T.M., and Edwards, M.A., 2004, Late Miocene movement within the Himalayan Main Central Thrust shear zone, Sikkim, north-east India: Journal of Metamorphic Geology, v. 22, p. 207–226. doi:10.1111/j.1525-1314.2004.00509.x

Catlos, E.J., Harrison, T.M., Kohn, M.J., Grove, M., Ryerson, F. J., Manning, C.E., and Upreti, B.N., 2001, Geochronologic and thermobarometric constraints on the evolution of the Main Central Thrust, central Nepal Himalaya: Journal of Geophysical Research, v. 106, p. 16177–16204. doi:10.1029/2000JB900375

Célérier, J., Harrison, T.M., Webb, A.A.G., and Yin, A., 2009, The Kumaun and Garwhal Lesser Himalaya, India: Part 1. Structure and stratigraphy: Geological Society of America Bulletin, v. 121, p. 1262–1280. doi:10.1130/B26344.1

Chambers, J., Caddick, M., Argles, T., Horstwood, M., Sherlock, S., Harris, N., Parrish, R., and Ahmad, T., 2009, Empirical constraints on extrusion mechanisms from the upper margin of an exhumed high-grade orogenic core, Sutlej valley, NW India: Tectonophysics, v. 477, p. 77–92. doi:10.1016/j.tecto.2008.10.013

Chen, Z., Liu, Y., Hodges, K.V., Burchfiel, B.C., Royden, L.H., and Deng, C., 1990, The Kangmar dome: A metamorphic core complex in southern Xizang (Tibet): Science, v. 250, p. 1552–1556. doi:10.1126/science.250.4987.1552

Colchen, M., Le Fort, P., and Pêcher, A., 1986, Annapurna–Manaslu–Ganesh Himal: Paris, Centre National de la Recherche Scientifique, p. 136.

Corfu, F., Hanchar, J.M., Hoskin, P.W.O., and Kinny, P., 2003, Atlas of zircon textures: Reviews in Mineralogy and Geochemistry, v. 53, p. 469–500. doi:10.2113/0530469

Corrie, S.L., and Kohn, M.J., 2011, Metamorphic history of the central Himalaya, Annapurna region, Nepal, and implications for tectonic models: Geological Society of America Bulletin, v. 123, p. 1863–1879. doi:10.1130/B30376.1

Corrie, S.L., Kohn, M.J., McQuarrie, N., and Long, S.P., 2012, Flattening the Bhutan Himalaya: Earth and Planetary Science Letters, v. 349-350, p. 67–74. doi:10.1016/j.epsl.2012.07.001

Cottle, J.M., Jessup, M.J., Newell, D.L., Searle, M.P., Law, R.D., and Horstwood, M.S.A., 2007, Structural insights into the early stages of exhumation along an orogen-scale detachment: The South Tibetan Detachment System, Dzakaa Chu section, Eastern Himalaya: Journal of Structural Geology, v. 29, p. 1781–1797. doi:10.1016/j.jsg.2007.08.007

Cottle, J.M., Searle, M.P., Horstwood, M.S.A., and Waters, D., 2009, Timing of midcrustal metamorphism, melting, and deformation in the Mount Everest region of Southern Tibet revealed by U(-Th)-Pb geochronology: The Journal of Geology, v. 117, p. 643–664. doi:10.1086/605994

Cottle, J.M., Waters, D.J., Riley, D., Beyssac, O., and Jessup, M. J., 2011, Metamorphic history of the South Tibetan Detachment System, Mt. Everest region, revealed by RSCM thermometry and phase equilibria modelling: Journal of Metamorphic Geology, v. 29, p. 561–582. doi:10.1111/j.1525-1314.2011.00930.x

Davis, D., Suppe, J., and Dahlen, F.A., 1983, Mechanics of fold-and-thrust belts and accretionary wedges: Journal of Geophysical Research, v. 88, p. 1153–1178. doi:10.1029/JB088iB02p01153

DeCelles, P.G., Gehrels, G.E., Quade, J., LaReau, B., and Spurlin, M., 2000, Tectonic implications of U-Pb zircon ages of the Himalayan orogenic belt in Nepal: Science, v. 288, p. 497–499. doi:10.1126/science.288.5465.497

DeCelles, P.G., Robinson, D.M., Quade, J., Ojha, T.P., Garzione, C.N., Copeland, P., and Upreti, B.N., 2001, Stratigraphy, structure, and tectonic evolution of the Himalayan fold-thrust belt in western Nepal: Tectonics, v. 20, p. 487–509. doi:10.1029/2000TC001226

Dunne, W.M., and Ferrill, D.A., 1988, Blind thrust systems: Geology, v. 16, p. 33–36. doi:10.1130/0091-7613(1988)016<0033:BTS>2.3.CO;2

Edwards, M.A., Kidd, W.S.F., Li, J., Yue, Y., and Clark, M., 1996, Multi-stage development of the southern Tibet detachment system near Khula Kangri: New data from Gonto La: Tectonophysics, v. 260, p. 1–19. doi:10.1016/0040-1951(96)00073-X

Epard, J.L., and Steck, A., 2004, The Eastern prolongation of the Zanskar Shear Zone (Western Himalaya): Eclogae Geologicae Helvetiae, v. 97, p. 193–212. doi:10.1007/s00015-004-1116-7

Erickson, S.G., 1995, Mechanics of triangle zones and passive-roof duplexes: Implications of finite-element models: Tectonophysics, v. 245, p. 1–11. doi:10.1016/0040-1951(94)00251-4

Faccenda, M., Gerya, T.V., and Chakraborty, S., 2008, Styles of post-subduction collisional orogeny: Influence of convergence velocity, crustal rheology and radiogenic heat production: Lithos, v. 103, p. 257–287. doi:10.1016/j.lithos.2007.09.009

Frank, W., Grasemann, B., Guntli, P., and Miller, C., 1995, Geological map of the Kishtwar–Chamba–Kulu region (NW Himalayas, India): Jahrbuch Der Geologischen Bundesanstalt, v. 138, p. 208–299.

Fuchs, G., and Linner, M., 1995, Geological traverse across the western Himalaya: A contribution to the geology of eastern Ladakh, Lahul, and Chamba: Jahrbuch der Geologischen Bundesanstalt Wien, v. 138, p. 655–685.

Gehrels, G.E., DeCelles, P.G., Martin, A., Ojha, T.P., Pinhassi, G., and Upreti, B.N., 2003, Initiation of the Himalayan orogen as an early Paleozoic thin-skinned thrust belt: GSA Today, v. 13, p. 4–9. doi:10.1130/1052-5173(2003)13<4:IOTHOA>2.0.CO;2

Gehrels, G.E., DeCelles, P.G., Ojha, T.P., and Upreti, B.N., 2006, Geologic and U-Th-Pb geochronologic evidence for early Paleozoic tectonism in the Kathmandu thrust sheet, central Nepal Himalaya: Geological Society of America Bulletin, v. 118, p. 185–198. doi:10.1130/B25753.1

Godin, L., 2003, Structural evolution of the Tethyan sedimentary sequence in the Annapurna area, central Nepal Himalaya: Journal of Asian Earth Sciences, v. 22, p. 307–328. doi:10.1016/S1367-9120(03)00066-X

Godin, L., Brown, R.L., and Hanmer, S., 1999, High strain zone in the hanging wall of the Annapurna detachment, central Nepal Himalaya, *in* Macfarlane, A., Sorkhabi, R.B., and Quade, J., eds., Himalaya and Tibet: Mountain roots to mountain tops: Geological Society of America Special Papers 328, p. 199–210.

Godin, L., Grujic, D., Law, R., and Searle, M.P., 2006, Crustal flow, extrusion, and exhumation in continental collision zones: An introduction, *in* Law, R., Searle, M.P., and Godin, L., eds., Channel flow, ductile extrusion, and exhumation in continental collision zones: Geological Society, London, Special Publication 268, p. 1–23.

Godin, L., Parrish, R.R., Brown, R.L., and Hodges, K.V., 2001, Crustal thickening leading to exhumation of the Himalayan metamorphic core of central Nepal: Insight from U-Pb geochronology and $^{40}Ar/^{39}Ar$ thermochronology: Tectonics, v. 20, p. 729–747. doi:10.1029/2000TC001204

Goscombe, B., Gray, D., and Hand, M., 2006, Crustal architecture of the Himalayan metamorphic front in eastern Nepal: Gondwana Research, v. 10, p. 232–255. doi:10.1016/j.gr.2006.05.003

Goscombe, B., and Hand, M., 2000, Contrasting P-T paths in the Eastern Himalaya, Nepal: Inverted isograds in a paired metamorphic mountain belt: Journal of Petrology, v. 41, p. 1673–1719. doi:10.1093/petrology/41.12.1673

Grandin, R., Doin, M.-P., Bollinger, L., Pinel-Puyssegur, B., Ducret, G., Jolivet, R., and Sapkota, S.N., 2012, Long-term growth of the Himalaya inferred from interseismic InSAR measurement: Geology, v. 40, p. 1059–1062. doi:10.1130/G33154.1

Grujic, D., 2006, Channel flow and continental collision tectonics: An overview, in Law, R.D., Searle, M.P., and Godin, L., eds., Channel flow, ductile extrusion and exhumation in continental collision zones: Geological Society, London, Special Publication 268, p. 25–37.

Grujic, D., Hollister, L.S., and Parrish, R.R., 2002, Himalayan metamorphic sequence as an orogenic channel: Insight from Bhutan: Earth and Planetary Science Letters, v. 198, p. 177–191. doi:10.1016/S0012-821X(02)00482-X

Grujic, D., Warren, C.J., and Wooden, J.L., 2011, Rapid synconvergent exhumation of Miocene-aged lower orogenic crust in the eastern Himalaya: Lithosphere, v. 3, p. 346–366. doi:10.1130/L154.1

Hagen, T., 1969, Report on the geological survey of Nepal: Volume 1: Preliminary reconnaissance: Zurich, Social Helvétique Sciences Natural Mém, v. 86, p. 185.

Harris, N., 2007, Channel flow and the Himalayan-Tibetan orogen: A critical review: Journal of the Geological Society, v. 164, p. 511–523. doi:10.1144/0016-76492006-133

Harrison, T.M., Grove, M., Lovera, O.M., and Catlos, E.J., 1998, A model for the origin of Himalayan anatexis and inverted metamorphism: Journal of Geophysical Research, v. 103, p. 27017–27032. doi:10.1029/98JB02468

Harrison, T.M., Ryerson, F.J., Le Fort, P., Yin, A., Lovera, O.M., and Catlos, E.J., 1997, A late Miocene-Pliocene origin for the Central Himalayan inverted metamorphism: Earth and Planetary Science Letters, v. 146, p. E1–E7. doi:10.1016/S0012-821X(96)00215-4

Hayashi, D., Fujii, Y., Yoneshiro, T., and Kizaki, K., 1984, Observations on the geology of the Karnali Region, West Nepal: Journal Nepal Geological Society, v. 4, p. 29–40.

He, D., Webb, A.A.G., Larson, K.P., and Schmitt, A.K., 2014, Extrusion vs. duplexing models of Himalayan mountain building 2: The South Tibet detachment at the Dadeldhura klippe: Tectonophysics (in review).

Herman, F., Copeland, P., Avouac, J.-P., Bollinger, L., Mahéo, G., Le Fort, P., Rai, S., Foster, D., Pêcher, A., Stüwe, K., and Henry, P., 2010, Exhumation, crustal deformation, and thermal structure of the Nepal Himalaya derived from the inversion of thermochronological and thermobarometric data and modeling of the topography: Journal of Geophysical Research, v. 115. doi:10.1029/2008JB006126.

Hodges, K.V., 2000, Tectonics of the Himalaya and southern Tibet from two perspectives: Geological Society of America Bulletin, v. 112, p. 324–350. doi:10.1130/0016-7606(2000)112<324:TOTHAS>2.0.CO;2

Hodges, K.V., Hurtado, J.M., and Whipple, K.X., 2001, Southward extrusion of Tibetan crust and its effect on Himalayan tectonics: Tectonics, v. 20, p. 799–809. doi:10.1029/2001TC001281

Hodges, K.V., Parrish, R.R., Housh, T.B., Lux, D.R., Burchfiel, B. C., Royden, L.H., and Chen, Z., 1992, Simultaneous Miocene extension and shortening in the Himalayan orogen: Science, v. 258, p. 1466–1470. doi:10.1126/science.258.5087.1466

Hodges, K.V., Parrish, R.R., and Searle, M.P., 1996, Tectonic evolution of the central Annapurna Range, Nepalese Himalayas: Tectonics, v. 15, p. 1264–1291. doi:10.1029/96TC01791

Hodges, K.V., Wobus, C., Ruhl, K., Schildgen, T., and Whipple, K., 2004, Quaternary deformation, river steepening, and heavy precipitation at the front of the Higher Himalayan ranges: Earth and Planetary Science Letters, v. 220, p. 379–389. doi:10.1016/S0012-821X(04)00063-9

Hoskin, P.W.O., and Black, L.P., 2000, Metamorphic zircon formation by solid-state recrystallization of protolith igneous zircon: Journal of Metamorphic Geology, v. 18, p. 423–439. doi:10.1046/j.1525-1314.2000.00266.x

Hurtado, J.M., Hodges, K.V., and Whipple, K.X., 2001, Neotectonics of the Thakkhola graben and implications for recent activity on the South Tibetan fault system in the central Nepal Himalaya: Geological Society of America Bulletin, v. 113, p. 222–240. doi:10.1130/0016-7606(2001)113<0222:NOTTGA>2.0.CO;2

Imayama, T., Takeshita, T., Yi, K., Cho, D.-L., Kitajima, K., Tsutsumi, Y., Kayama, M., Nishido, H., Okumura, T., Yagi, K., Itaya, T., and Sano, Y., 2012, Two-stage partial melting and contrasting cooling history within the Higher Himalayan Crystalline Sequence in the far-eastern Nepal Himalaya: Lithos, v. 134-135, p. 1–22. doi:10.1016/j.lithos.2011.12.004

Inger, S., and Harris, N.B.W., 1992, Tectonothermal evolution of the High Himalayan Crystalline Sequence, Langtang Valley, northern Nepal: Journal of Metamorphic Geology, v. 10, p. 439–452.

Jamieson, R.A., and Beaumont, C., 2013, On the origin of orogens: Geological Society of America Bulletin, v. 125, p. 1671–1702. doi:10.1130/B30855.1

Jamieson, R.A., Beaumont, C., Medvedev, S., and Nguyen, M. H., 2004, Crustal channel flows: 2. Numerical models with implications for metamorphism in the Himalayan-Tibetan orogen: Journal of Geophysical Research, v. 109, p. B6. doi:10.1029/2003JB002811.

Jessup, M.J., Cottle, J.M., Searle, M.P., Law, R.D., Newell, D.L., Tracy, R.J., and Waters, D.J., 2008, P-T-t-D paths of Everest series schist, Nepal: Journal of Metamorphic Geology, v. 26, p. 717–739. doi:10.1111/j.1525-1314.2008.00784.x

Johnson, M.R.W., 2005, Structural settings for the contrary metamorphic zonal sequences in the internal and external zones of the Himalaya: Journal of Asian Earth Sciences, v. 25, p. 695–706. doi:10.1016/j.jseaes.2004.04.010

Johnson, M.R.W., Oliver, G.J.H., Parrish, R.R., and Johnson, S. P., 2001, Synthrusting metamorphism, cooling, and erosion of the Himalayan Kathmandu complex, Nepal: Tectonics, v. 20, p. 394–415. doi:10.1029/2001TC900005

Johnson, M.R.W., and Rogers, G., 1997, Rb-Sr ages of micas from the Kathmandu Complex, Central Nepalese Himalaya: Implications for the evolution of the Main Central Thrust: Journal of the Geological Society of London, v. 154, p. 863–869. doi:10.1144/gsjgs.154.5.0863

Jones, P.B., 1996, Triangle zone geometry, terminology and kinematics: Bulletin of Canadian Petroleum Geology, v. 44, p. 139–152.

Kali, E., Leloup, P.H., Arnaud, N., Mahéo, G., Liu, D., Boutonnet, E., Van Der Woerd, J., Liu, X., Liu-Zeng, J., and Li, H., 2010, Exhumation history of the deepest central Himalayan rocks, Ama Drime range: Key pressure-temperature-deformation-time constraints on orogenic models: Tectonics, v. 29, p. TC2014. doi:10.1029/2009TC002551.

Kellett, D.A., and Godin, L., 2009, Pre-Miocene deformation of the Himalayan superstructure, Hidden valley, central Nepal: Journal of the Geological Society of London, v. 166, p. 261–275. doi:10.1144/0016-76492008-097

Kellett, D.A., and Grujic, D., 2012, New insight into the South Tibetan detachment system: Not a single progressive deformation: Tectonics, v. 31, p. TC2007. doi:10.1029/2011TC002957

Kellett, D.A., Grujic, D., Warren, C., Cottle, J., Jamieson, R., and Tenzin, T., 2010, Metamorphic history of a syn-convergent orogen-parallel detachment: The South Tibetan detachment system, Bhutan Himalaya: Journal of Metamorphic Geology, v. 28, p. 785–808. doi:10.1111/j.1525-1314.2010.00893.x

Khanal, S., and Robinson, D.M., 2013, Upper crustal shortening and forward modeling of the Himalayan thrust belt along the Budhi-Gandaki River, central Nepal: International Journal of Earth Sciences, v. 102, p. 1871–1891. doi:10.1007/s00531-013-0889-1

Khanal, S., Robinson, D.M., and Kohn, M.J., 2014, Evidence for a far traveled thrust sheet in the Greater Himalayan thrust system, and an alternative model to building the Himalaya: Tectonics (in press).

King, J., Harris, N., Argles, T., Parrish, R., and Zhang, H., 2011, Contribution of crustal anatexis to the tectonic evolution of Indian crust beneath southern Tibet: Geological Society of America Bulletin, v. 123, p. 218–239. doi:10.1130/B30085.1

Kohn, M.J., 2008, PTt data from central Nepal support critical taper and repudiate large-scale channel flow of the Greater Himalayan Sequence: Geological Society of America Bulletin, v. 120, p. 259–273. doi:10.1130/B26252.1

Kohn, M.J., Wieland, M.S., Parkinson, C.D., and Upreti, B.N., 2004, Miocene faulting at plate tectonic velocity in the Himalaya of central Nepal: Earth and Planetary Science Letters, v. 228, p. 299–310. doi:10.1016/j.epsl.2004.10.007

Konstantinovskaia, E., and Malavieille, J., 2005, Erosion and exhumation in accretionary orogens: Experimental and geological approaches: Geochemistry Geophysics Geosystems, v. 6. doi:10.1029/2004GC000794.

Kruhl, J.H., 1998, Prism- and basal-plane parallel subgrain boundaries in quartz: A microstructural geothermobarometer – Reply: Journal of Metamorphic Geology, v. 16, p. 142–146.

Larson, K.P., and Cottle, J.M., 2014, Midcrustal discontinuities and the assembly of the Himalayan mid-crust: Tectonics (in press). doi:10.1002/2013TC003452

Larson, K.P., Gervais, F., and Kellett, D.A., 2013, A P-T-t-D discontinuity in east-central Nepal: Implications for the evolution of the Himalayan mid-crust: Lithos, v. 179, p. 275–292. doi:10.1016/j.lithos.2013.08.012

Larson, K.P., and Godin, L., 2009, Kinematics of the Greater Himalayan Sequence, Dhaulagiri Himal: Implications for the structural framework of central Nepal: Journal of the Geological Society, v. 166, p. 25–43. doi:10.1144/0016-76492007-180

Larson, K.P., Godin, L., Davis, W.J., and Davis, D.W., 2010a, Out-of-sequence deformation and expansion of the Himalayan orogenic wedge: Insight from the Changgo culmination, south central Tibet: Tectonics, v. 29, p. TC4013. doi:10.1029/2008TC002393.

Larson, K.P., Godin, L., and Price, R.A., 2010b, Relationships between displacement and distortion in orogens: Linking the Himalayan foreland and hinterland in central Nepal: Geological Society of America Bulletin, v. 122, p. 1116–1134. doi:10.1130/B30073.1

Lavé, J., and Avouac, J.P., 2000, Active folding of fluvial terraces across the Siwaliks Hills, Himalayas of central Nepal: Journal of Geophysical Research, v. 105, p. 5735–5770. doi:10.1029/1999JB900292

Law, R.D., 1990, Crystallographic fabrics: A selective review of their applications to research in structural geology, *in* Knipe, R.J., and Rutter, E.H., eds., Deformation mechanisms, rheology and tectonics: Geological Society Special Publication 54, p. 335–352.

Law, R.D., Jessup, M.J., Searle, M.P., Francsis, M.K., Waters, D. J., and Cottle, J.M., 2011, Telescoping of isotherms beneath the South Tibetan Detachment System, Mount Everest Massif: Journal of Structural Geology, v. 33, p. 1569–1594. doi:10.1016/j.jsg.2011.09.004

Law, R.D., Searle, M.P., and Simpson, R.L., 2004, Strain, deformation temperatures and vorticity of flow at the top of the Greater Himalayan Slab, Everest massif, Tibet: Journal of the Geological Society of London, v. 161, p. 305–320. doi:10.1144/0016-764903-047

Law, R.D., Stahr, D.W., Francsis, M.K., Grasemann, B., and Ahmad, T., 2013, Deformation temperatures and flow vorticities near the base of the Greater Himalayan Series, Sutlej Valley and Shimla klippe, NW India: Journal of Structural Geology, v. 54, p. 21–53. doi:10.1016/j.jsg.2013.05.009

Le Fort, P., 1975, Himalayas: The collided range. Present knowledge of the continental arc: American Journal of Science, v. A275, p. 1–44.

Lee, J., Hacker, B.R., and Wang, Y., 2004, Evolution of North Himalayan gneiss domes: Structural and metamorphic studies in Mabja Dome, southern Tibet: Journal of Structural Geology, v. 26, p. 2297–2316. doi:10.1016/j.jsg.2004.02.013

Lee, J., and Whitehouse, M.J., 2007, Onset of mid-crustal extensional flow in southern Tibet: Evidence from U/Pb zircon ages: Geology, v. 35, p. 45–48. doi:10.1130/G22842A.1

Leger, R.M., Webb, A.A.G., Henry, D.J., Graig, J.A., and Dubey, P., 2013, Metamorphic field gradients across the Himachal Himalaya, northwest India: Implications for the emplacement of the Himalayan crystalline core: Tectonics, v. 32, p. 540–557. doi:10.1002/tect.20020

Lister, G.S., and Hobbs, B.E., 1980, The simulation of fabric development during plastic deformation and its application to quartzite: The influence of deformation history: Journal of Structural Geology, v. 2, p. 355–370. doi:10.1016/0191-8141(80)90023-1

Lister, G.S., and Price, G.P., 1978, Fabric development in a quartz-feldspar mylonite: Tectonophysics, v. 49, p. 37–78. doi:10.1016/0040-1951(78)90097-5

Lombardo, B., Pertusati, P., and Borghi, S., 1993, Geology and tectonomagmatic evolution of the eastern Himalaya along the Chomolungma-Makalu transect, *in* Treloar, P.J., and Searle, M.P., eds., Himalayan tectonics: Geological Society London Special Publication 74, p. 341–355.

Long, S., and McQuarrie, N., 2010, Placing limits on channel flow: Insights from the Bhutan Himalaya: Earth and Planetary Science Letters, v. 290, p. 375–390. doi:10.1016/j.epsl.2009.12.033

Long, S., McQuarrie, N., Tobgay, T., and Grujic, D., 2011, Geometry and crustal shortening of the Himalayan fold-thrust belt, eastern and central Bhutan: Geological Society of America Bulletin, v. 123, p. 1427–1447. doi:10.1130/B30203.1

Macfarlane, A.M., 1993, Chronology of tectonic events in the crystalline core of the Himalaya, Langtang National Park, central Nepal: Tectonics, v. 12, p. 1004–1025. doi:10.1029/93TC00916

Martin, A.J., Copeland, P., and Benowitz, J.A., 2014, Muscovite $^{40}Ar/^{39}Ar$ ages help reveal the Neogene tectonic evolution of the southern Annapurna Range, central Nepal, *in* Mukherjee, S., Carosi, R., van der Beek, P.A., Mukherjee, B.K., and Robinson, D., eds., Tectonics of the Himalaya: Geological Society of London Special Publication, 412. doi:10.1144/SP412.5.

Martin, A.J., DeCelles, P.G., Gehrels, G.E., Patchett, P.J., and Isachsen, C., 2005, Isotopic and structural constraints on the location of the Main Central thrust in the Annapurna Range, central Nepal Himalaya: Geological Society of America Bulletin, v. 117, p. 926–944.

Martin, A.J., Ganguly, J., and DeCelles, P.G., 2010, Metamorphism of Greater and Lesser Himalayan rocks exposed in the Modi Khola valley, central Nepal: Contributions to Mineralogy and Petrology, v. 159, p. 203–223. doi:10.1007/s00410-009-0424-3

McDermott, J.A., Whipple, K.X., Hodges, K.V., and Van Soest, M.C., 2013, Evidence for Plio-Pleistocene north-south extension at the southern margin of the Tibetan Plateau, Nyalam region: Tectonics, v. 32, p. 317–333. doi:10.1002/tect.20018

McElroy, R., Cater, J., Roberts, I., Peckham, A., and Bond, M., 1990, The structure and stratigraphy of SE Zanskar, Ladakh Himalaya: Journal of the Geological Society, v. 147, p. 989–997. doi:10.1144/gsjgs.147.6.0989

McQuarrie, N., Robinson, D., Long, S., Tobgay, T., Grujic, D., Gehrels, G., and Ducea, M., 2008, Preliminary stratigraphic and structural architecture of Bhutan: Implications for the along strike architecture of the Himalayan system: Earth and Planetary Science Letters, v. 272, p. 105–117. doi:10.1016/j.epsl.2008.04.030

McQuarrie, N., Tobgay, T., Long, S.P., Reiners, P.W., and Cosca, M.A., 2014, Variable exhumation rates and variable displacement rates: Documenting recent slowing of Himalayan shortening in western Bhutan: Earth and Planetary Science Letters, v. 386, p. 161–174. doi:10.1016/j.epsl.2013.10.045

Metcalfe, R.P., 1993, Pressure, temperature and time constraints on metamorphism across the Main Central Thrust zone and High Himalayan slab in the Garhwal Himalaya, *in* Treloar, P.J., and Searle, M.P., eds., Himalayan Tectonics: The Geological Society Special Publication 74, p. 485–509.

Montomoli, C., Iaccarino, S., Carosi, R., Langone, A., and Visonà, D., 2013, Tectonometamorphic discontinuities within the Greater Himalayan Sequence in Western Nepal (Central Himalaya): Insights on the exhumation of crystalline rocks: Tectonophysics, v. 608, p. 1349–1370. doi:10.1016/j.tecto.2013.06.006

Mukherjee, S., Koyi, H.A., and Talbot, C.J., 2012, Implications of channel flow analogue models for extrusion of the Higher Himalayan Shear Zone with special reference to the out-of-sequence thrusting: International Journal of Earth Sciences, v. 101, p. 253–272. doi:10.1007/s00531-011-0650-6

Murphy, M.A., 2007, Isotopic characteristics of the Gurla Mandhata metamorphic core complex: Implications for the architecture of the Himalayan orogen: Geology, v. 35, p. 983–986. doi:10.1130/G23774A.1

Murphy, M.A., and Copeland, P., 2005, Transtensional deformation in the central Himalaya and its role in accommodating growth of the Himalayan orogen: Tectonics, v. 24, p. TC4012. doi:10.1029/2004TC001659

Murphy, M.A., Saylor, J.E., and Ding, L., 2009, Late Miocene topographic inversion in southwest Tibet based on integrated paleoelevation reconstructions and structural history: Earth and Planetary Science Letters, v. 282, p. 1–9. doi:10.1016/j.epsl.2009.01.006

Murphy, M.A., and Yin, A., 2003, Structural evolution and sequence of thrusting in the Tethyan fold-thrust belt and Indus-Yalu suture zone, southwest Tibet: Geological Society of America Bulletin, v. 115, p. 21–34. doi:10.1130/0016-7606(2003)115<0021:SEASOT>2.0.CO;2

Nábělek, J., Hetenyi, G., Vergne, J., Sapkota, S., Kafle, B., Jiang, M., Su, H., Chen, J., Huang, B.-S., and Team, T.H.-C., and the Hi-CLIMB Team. 2009, Underplating in the Himalaya-Tibet collision zone revealed by the Hi-CLIMB experiment: Science, v. 325, p. 1371–1374. doi:10.1126/science.1167719

Nelson, K.D., Zhao, W., Brown, L.D., Kuo, J., Che, J., Liu, X., Klemperer, S.L., Makovsky, Y., Meissner, R., Mechie, J., Kind, R., Wenzel, F., Ni, J., Nabelek, J., Leshou, C., Tan, H., Wei, W., Jones, A.G., Booker, J., Unsworth, M., Kidd, W.S.F., Hauck, M., Alsdorf, D., Ross, A., Cogan, M., Wu, C., Sandvol, E., and Edwards, M., 1996, Partially molten middle crust beneath Southern Tibet: Synthesis of project INDEPTH results: Science, v. 274, p. 1684–1688. doi:10.1126/science.274.5293.1684

Paces, J.B., and Miller, J.D., 1993, Precise U-Pb ages of Duluth Complex and related mafic intrusions, northeastern Minnesota: Geochronological insights to physical, petrogenetic, paleomagnetic, and tectonomagmatic processes associated with the 1.1 Ga Midcontinent Rift System: Journal of Geophysical Research, v. 98, p. 13997–14013. doi:10.1029/93JB01159

Parrish, R.R., and Hodges, K.V., 1996, Isotopic constraints on the age and provenance of the Lesser and Greater Himalayan Sequences, Nepalese Himalaya: Geological Society of America Bulletin, v. 108, p. 904–911. doi:10.1130/0016-7606(1996)108<0904:ICOTAA>2.3.CO;2

Patino Douce, A.E., and Harris, N., 1998, Experimental constraints on Himalayan Anatexis: Journal of Petrology, v. 39, p. 689–710. doi:10.1093/petroj/39.4.689

Pecher, A., 1989, The metamorphism in the central Himalaya: Journal of Metamorphic Geology, v. 7, p. 31–41. doi:10.1111/j.1525-1314.1989.tb00573.x

Peternell, M., Hasalová, P., Wilson, C.J.L., Piazolo, S., and Schulmann, K., 2010, Evaluating quartz crystallographic preferred orientations and the role of deformation partitioning using EBSD and fabric analyser techniques: Journal of Structural Geology, v. 32, p. 803–817. doi:10.1016/j.jsg.2010.05.007

Quigley, M., Liangjun, L., Xiaohan, L., Wilson, C.J.L., Sandiford, M., and Phillips, D., 2006, 40Ar/39Ar thermochronology of the Kampa Dome, southern Tibet: Implications for tectonic evolution of the North Himalayan

gneiss domes: Tectonophysics, v. 421, p. 269–297. doi:10.1016/j.tecto.2006.05.002

Rai, S.M., Guillot, S., Le Fort, P., and Upreti, B.N., 1998, Pressure-temperature evolution in the Kathmandu and Gosainkund regions, Central Nepal: Journal of Asian Earth Sciences, v. 16, p. 283–298. doi:10.1016/S0743-9547(98)00019-1

Ratschbacher, L., Frisch, W., Liu, G., and Chen, C., 1994, Distributed deformation in southern and western Tibet during and after the India-Asia collision: Journal of Geophysical Research, v. 99, p. 19917–19945. doi:10.1029/94JB00932

Reddy, S.M., Searle, M.P., and Massey, J.A., 1993, Structural evolution of the High Himalayan gneiss sequence, Langtang Valley, Nepal, *in* Treloar, P.J., and Searle, M.P., eds., Himalayan Tectonics: Geological Society London Special Publication 74, p. 375–389.

Regis, D., Warren, C.J., Young, D., and Roberts, N.M.W, 2014, Tectono-metamorphic evolution of the Jomolhari massif: Variations in timing of syn-collisional metamorphism across western Bhutan: Lithos, v. 190–191, p. 449–466. doi:10.1016/j.lithos.2014.01.001

Robinson, D.M., DeCelles, P.G., and Copeland, P., 2006, Tectonic evolution of the Himalayan thrust belt in western Nepal: Implications for channel flow models: Geological Society of America Bulletin, v. 118, p. 865–885. doi:10.1130/B25911.1

Robinson, D.M., DeCelles, P.G., Garzione, C.N., Pearson, O.N., Harrison, T.M., and Catlos, E.J., 2003, Kinematic model for the Main Central Thrust in Nepal: Geology, v. 31, p. 359–362. doi:10.1130/0091-7613(2003)031<0359:KMFTMC>2.0.CO;2

Robinson, D.M., and Pearson, O.N., 2013, Was Himalayan normal faulting triggered by initiation of the Ramgarh-Munsiari thrust and development of the Lesser Himalayan duplex?: International Journal of Earth Sciences, v. 102, p. 1773–1790. doi:10.1007/s00531-013-0895-3

Robyr, M., Epard, J.-L., and Korh, A.E., 2014, Structural, metamorphic and geochronological relations between the Zanskar Shear Zone and the Miyar Shear Zone (NW Indian Himalaya): Evidence for two distinct tectonic structures and implications for the evolution of the High Himalayan Crystalline of Zanskar: Journal of Asian Earth Sciences, v. 79, p. 1–15.

Rubatto, D., 2002, Zircon trace element geochemistry: Partitioning with garnet and the link between U–Pb ages and metamorphism: Chemical Geology, v. 184, p. 123–138. doi:10.1016/S0009-2541(01)00355-2

Rubatto, D., Chakraborty, S., and Dasgupta, S., 2013, Timescales of crustal melting in the Higher Himalayan Crystallines (Sikkim, Eastern Himalaya) inferred from trace element-constrained monazite and zircon chronology: Contributions to Mineralogy and Petrology, v. 165, p. 349–372. doi:10.1007/s00410-012-0812-y

Rubatto, D., Hermann, J., and Buick, I.S., 2006, Temperature and bulk composition control on the growth of monazite and zircon during low-pressure anatexis (Mount Stafford, Central Australia): Journal of Petrology, v. 47, p. 1973–1996. doi:10.1093/petrology/egl033

Sapkota, J., and Sanislav, I.V., 2013, Preservation of deep Himalayan PT conditions that formed during multiple events in garnet cores: Mylonitization produces erroneous results for rims: Tectonophysics, v. 587, p. 89–106. doi:10.1016/j.tecto.2012.10.029

Schelling, D., 1992, The tectonostratigraphy and structure of the eastern Nepal Himalaya: Tectonics, v. 11, p. 925–943. doi:10.1029/92TC00213

Schelling, D., and Arita, K., 1991, Thrust tectonics, crustal shortening, and the structure of the far-eastern Nepal Himalaya: Tectonics, v. 10, p. 851–862. doi:10.1029/91TC01011

Schmid, S.M., and Casey, M., 1986, Complete fabric analysis of some commonly observed quartz C-axis patterns: Geophysical Monograph, v. 36, p. 263–286.

Schmitt, A.K., Grove, M., Harrison, T.M., Lovera, O.M., Hulen, J., and Walters, M., 2003, The Geysers-Cobb Mountain Magma System, California (Part 1): U-Pb zircon ages of volcanic rocks, conditions of zircon crystallization and magma residence times: Geochimica Et Cosmochimica Acta, v. 67, p. 3423–3442. doi:10.1016/S0016-7037(03)00140-6

Searle, M.P., 2010, Low-angle normal faults in the compressional Himalayan orogen: Evidence from the Annapurna-Dhaulagiri Himalaya, Nepal: Geosphere, v. 6,, p. 296–315. doi:10.1130/GES00549.1

Searle, M.P., and Godin, L., 2003, The South Tibetan detachment and the Manaslu leucogranite: A structural reinterpretation and restoration of the Annapurna-Manaslu Himalaya, Nepal: The Journal of Geology, v. 111, p. 505–523. doi:10.1086/376763

Searle, M.P., Law, R., Godin, L., Larson, K.P., Streule, M.J., Cottle, J., and Jessup, M., 2008, Defining the Himalayan Main Central thrust in Nepal: Journal of the Geological Society, London, v. 165, p. 523–534. doi:10.1144/0016-76492007-081

Searle, M.P., Parrish, R.R., Hodges, K.V., Hurford, A., Ayres, M.W., and Whitehouse, M.J., 1997, Shisha Pangma leucogranite, South Tibetan Himalaya: Field relations, geochemistry, age, origin, and emplacement: The Journal of Geology, v. 105, p. 295–318. doi:10.1086/515924

Searle, M.P., Simpson, R.L., Law, R.D., Parrish, R.R., and Waters, D.J., 2003, The structural geometry, metamorphic and magmatic evolution of the Everest massif, High Himalaya of Nepal-South Tibet: Journal of the Geological Society, v. 160, p. 345–366. doi:10.1144/0016-764902-126

Srivastava, P., and Mitra, G., 1994, Thrust geometries and deep structure of the outer and lesser Himalaya, Kumaon and Garhwal (India): Implications for evolution of the Himalayan fold-and-thrust belt: Tectonics, v. 13, p. 89–109. doi:10.1029/93TC01130

Stacey, J.S., and Kramers, J.D., 1975, Approximation of terrestrial lead isotope evolution by a two-stage model: Earth and Planetary Science Letters, v. 26, p. 207–221. doi:10.1016/0012-821X(75)90088-6

Steck, A., Spring, L., Vannay, J.-C., Masson, H., Bucher, H., Stutz, E., Marchant, R., and Tieche, J.-C., 1993, The tectonic evolution of the Northwestern Himalaya in eastern Ladakh and Lahul, India, *in* Treloar, P.J., and Searle, M.P., eds., Himalayan tectonics: Geological Society of London Special Publication 74, p. 265–276.

Stöcklin, J., 1980, Geology of Nepal and its regional frame: Thirty-third William Smith lecture: Journal of the Geological Society, v. 137, p. 1–34. doi:10.1144/gsjgs.137.1.0001

Stöcklin, J., and Bhattarai, K.D., 1982, Photogeological map of part of central Nepal: Kathmandu, Ministry of Industry and Commerce, Department of Mines and Geology, scale 1:100, 000.

Styron, R.H., Taylor, M.H., and Murphy, M.A., 2011, Oblique convergence, arc-parallel extension, and the role of strike-slip faulting in the High Himalaya: Geosphere, v. 7, p. 582–596. doi:10.1130/GES00606.1

Thakur, V.C., and Rawat, B.S., 1992, Geologic map of Western Himalaya: Dehra Dun, India, Wadia Institute of Himalayan Geology, scale 1:1,000,000.

Thiede, R., Bookhagen, B., Arrowsmith, J.R., Sobel, E., and Strecker, M., 2004, Climatic control on rapid exhumation along the Southern Himalayan Front: Earth and Planetary Science Letters, v. 222, p. 791–806. doi:10.1016/j.epsl.2004.03.015

Thiede, R.C., and Ehlers, T.A., 2013, Large spatial and temporal variations in Himalayan denudation: Earth and Planetary Science Letters, v. 371-372, p. 278–293. doi:10.1016/j.epsl.2013.03.004

Thiede, R.C., Ehlers, T.A., Bookhagen, B., and Strecker, M.R., 2009, Erosional variability along the northwest Himalaya: Journal of Geophysical Research, v. 114. doi:10.1029/2008JF001010.

Tullis, J.A., Christie, J.M., and Griggs, D.T., 1973, Microstructures and preferred orientations of experimentally deformed quartzites: Geological Society of America Bulletin, v. 84, p. 297–314. doi:10.1130/0016-7606(1973)84<297:MAPOOE>2.0.CO;2

Upreti, B.N., 1999, An overview of the stratigraphy and tectonics of the Nepal Himalaya: Journal of Asian Earth Sciences, v. 17, p. 577–606. doi:10.1016/S1367-9120(99)00047-4

Upreti, B.N., and Le Fort, P., 1999, Lesser Himalayan crystalline nappes of Nepal: Problem of their origin, *in* Macfarlane, A., Quade, J., and Sorkhabi, R., eds., Himalaya and Tibet: Mountain roots to mountain tops: Geological Society of America Special Paper 328, p. 225–238.

Vannay, J.-C., and Grasemann, B., 2001, Himalayan inverted metamorphism and syn-convergence extension as a consequence of a general shear extrusion: Geological Magazine, v. 138, p. 253–276. doi:10.1017/S0016756801005313

Vannay, J.-C., Grasemann, B., Rahn, M., Frank, W., Carter, A., Baudraz, V., and Cosca, M., 2004, Miocene to Holocene exhumation of metamorphic crustal wedges in the NW Himalaya: Evidence for tectonic extrusion coupled to fluvial erosion: Tectonics, v. 23, p. TC1014. doi:10.1029/2002TC001429.

Vannay, J.-C., and Hodges, K.V., 1996, Tectonometamorphic evolution of the Himalayan metamorphic core between the Annapurna and Dhaulagiri, central Nepal: Journal of Metamorphic Geology, v. 14, p. 635–656. doi:10.1046/j.1525-1314.1996.00426.x

Vannay, J.-C., and Steck, A., 1995, Tectonic evolution of the High Himalaya in Upper Lahul (NW Himalaya, India): Tectonics, v. 14, p. 253–263. doi:10.1029/94TC02455

Wagner, T., Lee, J., Hacker, B.R., and Seward, G., 2010, Kinematics and vorticity in Kangmar Dome, southern Tibet: Testing mid-crustal channel flow models for the Himalaya: Tectonics, v. 29, p. TC6011. doi:10.1029/2010TC002746

Wang, J.M., Zhang, J.J., and Wang, X.X., 2013, Structural kinematics, metamorphic P–T profiles and zircon geochronology across the Greater Himalayan Crystalline Complex in south-central Tibet: Implication for a revised channel flow: Journal of Metamorphic Geology, v. 31, p. 607–628. doi:10.1111/jmg.12036

Warren, C.J., Grujic, D., Kellett, D.A., Cottle, J., Jamieson, R.A., and Ghalley, K.S., 2011, Probing the depths of the India-Asia collision: U-Th-Pb monazite chronology of granulites from NW Bhutan: Tectonics, v. 30, p. TC2004. doi:10.1029/2010TC002738

Warren, C.J., Singh, A.K., Roberts, N.M.W., Regis, D., Halton, A.M., and Singh, R.B., 2014, Timing and conditions of peak metamorphism and cooling across the Zimithang Thrust, Arunachal Pradesh, India: Lithos, v. 200–201, p. 94–110. doi:10.1016/j.lithos.2014.04.005

Webb, A.A.G., 2013, Preliminary balanced palinspastic reconstruction of Cenozoic deformation across the Himachal Himalaya (northwestern India): Geosphere, v. 9, p. 572–587. doi:10.1130/GES00787.1

Webb, A.A.G., Schmitt, A.K., He, D., and Weigand, E.L., 2011a, Structural and geochronological evidence for the leading edge of the Greater Himalayan Crystalline complex in the central Nepal Himalaya: Earth and Planetary Science Letters, v. 304, p. 483–495. doi:10.1016/j.epsl.2011.02.024

Webb, A.A.G., Yin, A., and Dubey, C.S., 2013, U-Pb zircon geochronology of major lithologic units in the eastern Himalaya: Implications for the origin and assembly of Himalayan rocks: Geological Society of America Bulletin, v. 125, p. 499–522. doi:10.1130/B30626.1

Webb, A.A.G., Yin, A., Harrison, T.M., Célérier, J., and Burgess, W.P., 2007, The leading edge of the Greater Himalayan Crystalline complex revealed in the NW Indian Himalaya: Implications for the evolution of the Himalayan Orogen: Geology, v. 35, p. 955–958. doi:10.1130/G23931A.1

Webb, A.A.G., Yin, A., Harrison, T.M., Célérier, J., Gehrels, G.E., Manning, C.E., and Grove, M., 2011b, Cenozoic tectonic history of the Himachal Himalaya (northwestern India) and its constraints on the formation mechanism of the Himalayan orogen: Geosphere, v. 7, p. 1013–1061. doi:10.1130/GES00627.1

Wiedenbeck, M., Hanchar, J.M., Peck, W.H., Sylvester, P., Valley, J., Whitehouse, M., Kronz, A., Morishita, Y., Nasdala, L., Fiebig, J., Franchi, I., Girard, J.-P., Greenwood, R.C., Hinton, R., Kita, N., Mason, P.R.D., Norman, M., Ogasawara, M., Piccoli, P.M., Rhede, D., Satoh, H., Schulz-Dobrick, B., Skar, O., Spicuzza, M.J., Terada, K., Tindle, A., Togashi, S., Vennemann, T., Xie, Q., and Zheng, Y.-F., 2004, Further characterisation of the 91500 zircon crystal: Geostandard and Geoanalysis Research, v. 28, p. 9–39. doi:10.1111/j.1751-908X.2004.tb01041.x

Wiesmayr, G., and Grasemann, B., 2002, Eohimalayan fold and thrust belt: Implications for the geodynamic evolution of the NW Himalaya (India): Tectonics, v. 21, p. 8–18. doi:10.1029/2002TC001363.

Wilson, C.J.L., Russell-Head, D.S., Kunze, K., and Viola, G., 2007, The analysis of quartz c-axis fabrics using a modified optical microscope: Journal of Microscopy, v. 227, p. 30–41. doi:10.1111/j.1365-2818.2007.01784.x

Wobus, C.W., Heimsath, A.M., Whipple, K.X., and Hodges, K.V., 2005, Active out-of-sequence thrust faulting in the central Nepalese Himalaya: Nature, v. 434, p. 1008–1011. doi:10.1038/nature03499

Wobus, C.W., Hodges, K.V., and Whipple, K.X., 2003, Has focused denudation sustained active thrusting at the Himalayan topographic front?: Geology, v. 31, p. 861–864. doi:10.1130/G19730.1

Wobus, C.W., Pringle, M., Whipple, K., and Hodges, K., 2008, A Late Miocene acceleration of exhumation in the Himalayan crystalline core: Earth and Planetary Science Letters, v. 269, p. 1–10. doi:10.1016/j.epsl.2008.02.019

Yakymchuk, C., and Godin, L., 2012, Coupled role of deformation and metamorphism in the construction of inverted metamorphic sequences: An example from far-northwest Nepal: Journal of Metamorphic Geology, v. 30, p. 513–535. doi:10.1111/j.1525-1314.2012.00979.x

Yin, A., 2004, Gneiss domes and gneiss dome systems: Geological Society of America Special Papers, v. 380, p. 1–14.

Yin, A., 2006, Cenozoic tectonic evolution of the Himalayan orogen as constrained by along-strike variation of structural geometry, exhumation history, and foreland sedimentation:

Earth-Science Reviews, v. 76, p. 1–131. doi:10.1016/j.earscirev.2005.05.004

Yin, A., Dubey, C.S., Kelty, T.K., Webb, A.A.G., Harrison, T.M., Chou, C.Y., and Célérier, J., 2010, Geologic correlation of the Himalayan orogen and Indian craton: Part 2. Structural geology, geochronology, and tectonic evolution of the Eastern Himalaya: Geological Society of America Bulletin, v. 122, p. 360–395. doi:10.1130/B26461.1

Yin, A., Harrison, T.M., Murphy, M.A., Grove, M., Nie, S., Ryerson, F.J., Feng, W.X., and Le, C.Z., 1999, Tertiary deformation history of southeastern and southwestern Tibet during the Indo-Asian collision: Geological Society of America Bulletin, v. 111, p. 1644–1664. doi:10.1130/0016-7606(1999)111<1644:TDHOSA>2.3.CO;2

Yu, H., Webb, A.A.G., and He, D., 2014, Extrusion vs. duplexing models of Himalayan mountain building 1: Discovery of the Pabbar thrust, northwestern Indian Himalaya: Tectonics (in revision).

Zhang, J., Santosh, M., Wang, X., Guo, L., Yang, X., and Zhang, B., 2012, Tectonics of the northern Himalaya since the India–Asia collision: Gondwana Research, v. 21, p. 939–960. doi:10.1016/j.gr.2011.11.004